antioxidants

MDPI

Review

CD36 in Diabetic Kidney Disease: Membrane Trafficking, Redox Injury, and Therapeutic Targeting

Honglin Chen [1], Caihong He [1,2] and Tingting Li [2,3,*]

[1] School of Traditional Chinese Medicine, Ningxia Medical University, Yinchuan 750004, China; 15170340591@163.com (H.C.); 18695540639@163.com (C.H.)
[2] Key Laboratory of Dryness Syndrome in Chinese Medicine, Ministry of Education, Ningxia Medical University, Yinchuan 750004, China
[3] Ningxia Key Laboratory of Integrated Traditional Chinese and Western Medicine for Prevention and Treatment of Regional High-Incidence Diseases, Ningxia Medical University, Yinchuan 750004, China
* Correspondence: nxltt7088@163.com

Abstract

Cluster of differentiation 36 (CD36) links lipid handling to ligand-induced signaling in diabetic kidney disease (DKD), but its contribution to injury varies with cell type and metabolic conditions. This narrative review evaluates the evidence connecting CD36 to redox injury by comparing experimental interventions, functional measurements, and rescue studies. In podocytes, RNA turnover and palmitoylation regulate receptor availability. Tubular studies link CD36 manipulation to oxidative metabolism, mitochondrial oxidant signaling, and inflammatory amplification of lipid peroxidation. Alternative uptake routes, discordant localization findings, and lipid accumulation without a full fibrotic phenotype argue against a uniformly harmful role for CD36. We propose a model in which receptor availability affects ligand handling and signaling, while intracellular lipid processing and peroxide defense shape susceptibility to injury. Evaluation of receptor-directed interventions should account for the cell and protein-substrate selectivity of trafficking regulators. Human studies identify candidate CD36 measurements for evaluation in defined diagnostic, prognostic and treatment-response settings. Combining cell-specific receptor perturbation and appropriate reconstitution controls with substrate tracing and defined redox measurements provides a framework for testing renal protection after diabetic injury has developed.

Keywords: CD36; diabetic kidney disease; oxidative stress; lipotoxicity; lipid peroxidation; membrane trafficking; podocyte; ferroptosis

Check for updates

Academic Editor: Edgar A. Jaimes

Received: 16 October 2026
Revised: 1 November 2026
Accepted: 4 November 2026
Published: 16 November 2026

Copyright: © 2026 by the authors. Licensee MDPI, Basel, Switzerland. This article is an open access article distributed under the terms and conditions of the Creative Commons Attribution (CC BY) license.

1. Introduction and Scope

Diabetic kidney disease (DKD) exposes renal cells to sustained metabolic and inflammatory stress. The consequences of excess lipid depend on its uptake, oxidation, storage, and export. Cluster of differentiation 36 (CD36) participates in fatty acid handling and ligand-triggered signaling, placing it at the interface between metabolic exposure and cellular injury. Understanding when these physiological functions contribute to injury is essential to evaluating CD36 as a therapeutic target [1–4].

Renal triglyceride accumulation persisted after *Cd36* deletion in a fasting model, whereas deletion in a diabetic model improved mitochondrial and injury outcomes [5,6]. These findings raise a central therapeutic question: under which metabolic conditions does CD36 function contribute to injury? Receptor abundance alone cannot answer this question.

Existing reviews cover CD36 in chronic kidney disease (CKD), renal lipotoxicity, hypoxia, oxidative stress, and lipid peroxidation [7–10]. Recent syntheses examine adaptive lipid storage, kidney–vascular interactions, and therapeutic lipid remodeling [11–13], while reviews of post-translational regulation already discuss acyl-protein thioesterase 1 (APT1)-dependent CD36 depalmitoylation [14,15]. What remains unclear is which of these mechanisms provide sufficient evidence to support selective targeting of CD36. The scope of overlapping reviews is compared in Supplementary Table S1.

We compare CD36 expression and localization with evidence from receptor perturbation and reconstitution in DKD [16–18]. Building on the mechanisms discussed in previous reviews [7,14,15], the conditional model relates receptor availability to substrate handling, ligand-triggered signaling, lipid processing and peroxide defense. It organizes concordant and discordant uptake, storage and injury outcomes into comparisons within defined renal cell populations: whether protection accompanies reduced substrate entry, persists despite unchanged measured uptake, or varies with the protein substrates affected by upstream regulators. Supplementary Table S1 identifies the overlap with previous reviews and the interpretive focus of this synthesis.

We conducted targeted supplementary online searches on 1 October 2026 to verify literature relevant to CD36 in DKD. Search terms combined CD36 with "diabetic kidney disease" or "diabetic nephropathy," with additional combinations addressing trafficking, palmitoylation or depalmitoylation, ferroptosis, and oxidative stress. Searches targeted PubMed-indexed records, PMC articles and original publisher websites, without a publication-date filter. Original studies examining CD36 regulation or function in DKD were prioritized. Non-DKD studies were included where they clarified receptor function, assay interpretation or model-dependent differences, with their experimental settings explicitly identified. Related reviews provided context for the present synthesis. Publications assessed only through indexed abstracts were identified.

Evidence is distinguished by the question addressed: association with CD36 expression or localization; functional effects of receptor perturbation; CD36 re-expression and the extent to which it restored the measured phenotype; and attribution of in vivo effects to defined renal cell populations. Pharmacological inhibition, genetic manipulation and intervention in upstream regulators are evaluated separately. Oxidant signals, lipid peroxidation and cell death are treated as distinct outcomes. Evidence supporting ferroptosis and evidence supporting CD36 dependence are assessed separately within each experimental system (Tables 2 and 4).

Figure 1 outlines the structure of the review, linking receptor regulation and experimental injury mechanisms with human evidence, therapeutic assessment, and the research priorities developed from their comparison.

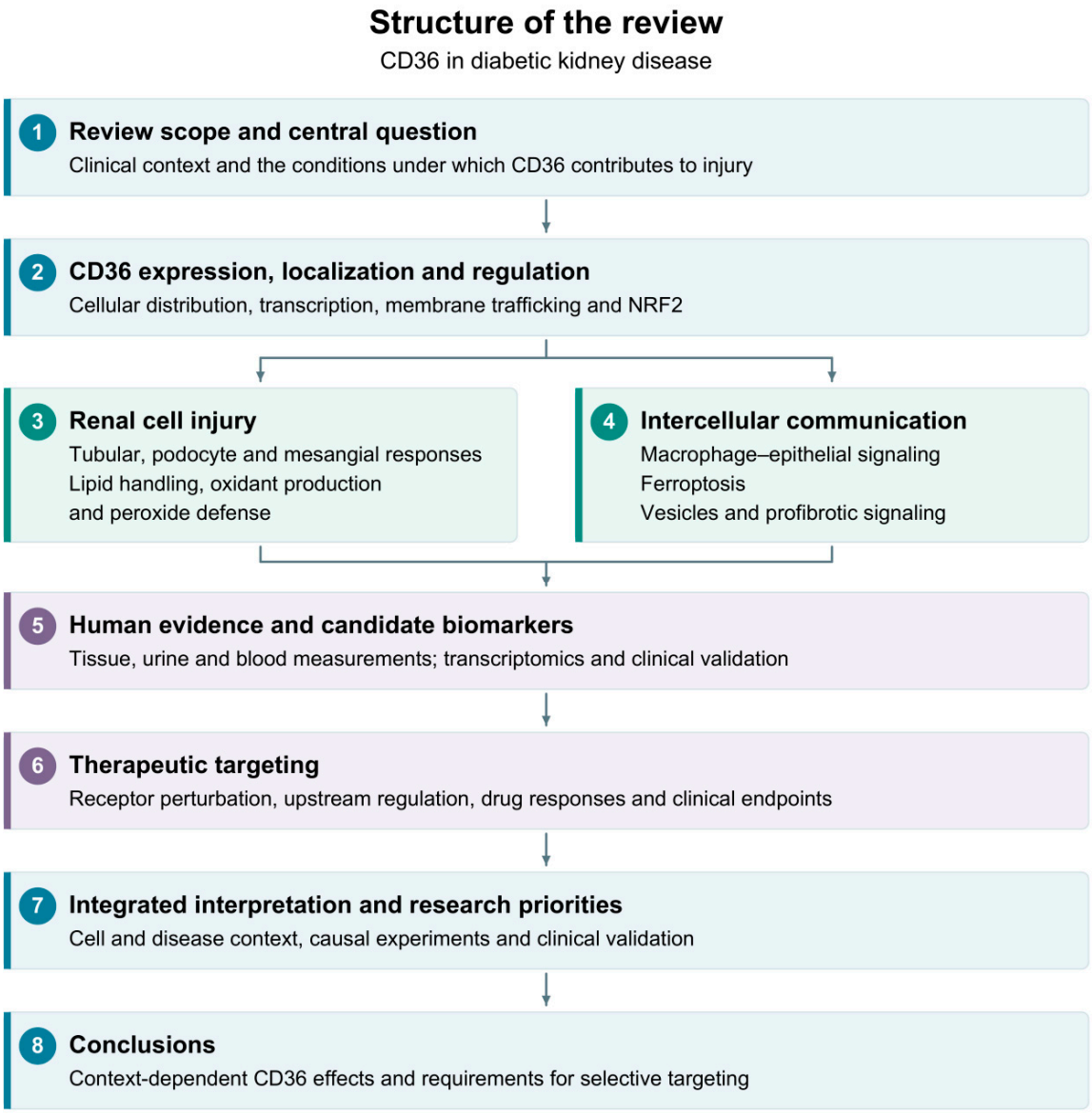


Figure 1. Structure and evidence flow of the review. The review moves from the review scope and central question (Section 1) to CD36 regulation (Section 2), followed by complementary assessments of renal cell injury and intercellular communication (Sections 3 and 4). Human evidence (Section 5) and therapeutic interventions (Section 6) inform the integrated interpretation and research priorities (Section 7) and conclusions (Section 8). Numbers identify manuscript sections. Arrows show the organization of the review, not biological causation or graded evidence certainty. CD36, cluster of differentiation 36; NRF2, nuclear factor erythroid 2-related factor 2.

2. Renal CD36 Expression, Localization, and Regulation

2.1. Cellular Distribution, Ligand Recognition, and Physiological Lipid Handling

CD36 is a membrane glycoprotein whose renal effects depend on cell identity and ligand exposure. Studies of diabetic kidney tissue and epithelial cell models implicate CD36 in fatty acid handling and signaling responses to modified lipoproteins and glycated proteins [19,20]. These functions must be assessed separately: ligand-triggered injury, substrate entry, and surface receptor abundance can change together or separately.

Ligand handling also differs between renal compartments. In an investigation comparing human podocytes with primary tubular cells, CD36 was principally involved in tubular

oxidized low-density lipoprotein (LDL) uptake, while C-X-C motif chemokine ligand 16 (CXCL16) accounted for much of the corresponding uptake in podocytes. Blocking CXCL16 reduced oxidized lipoprotein-associated oxidative stress and fibronectin production in the podocyte model. Consequently, podocyte uptake of an oxidized lipoprotein cannot automatically be attributed to CD36 merely because CD36 mediates tubular uptake of the same ligand [21].

In fasted mice, renal triglyceride accumulation tracked circulating nonesterified fatty acids, and *Cd36* deletion did not reduce oleate uptake or triglyceride accumulation [5]. This finding shows that CD36-independent uptake can sustain renal lipid storage in this non-diabetic setting.

An alternative route has been demonstrated in DKD by Mori and colleagues. Kidney injury molecule-1 (KIM-1) mediated proximal tubular uptake of albumin-bound palmitate in cultured epithelial cells. Deletion of its mucin domain reduced uptake in primary mouse tubular cells and attenuated renal injury in a diabetic model combining unilateral nephrectomy, a high-fat diet, and streptozotocin. The investigators did not detect CD36 in their KIM-1-expressing cell line or primary mouse proximal tubular cells. They also reported absent proximal tubular CD36 staining in the human DKD specimens examined, while interstitial staining provided a positive control [22]. KIM-1 therefore provides an alternative uptake route in this setting. The disagreement with positive tubular CD36 reports makes localization and disease context central to interpretation, as discussed in Section 7.1.

Complementing these uptake comparisons, inducible tubular CD36 overexpression increased lipid storage without producing a full fibrotic phenotype under the tested conditions [23]. The experimental context is discussed in Section 3.1.3.

Figure 2 summarizes these findings on uptake and lipid storage. Sections 2.2 and 2.3 examine how transcription and trafficking regulate CD36 availability.

2.2. Transcriptional Regulation of CD36 and Upstream RNA Modifications

High glucose can increase CD36 abundance through signaling pathways associated with transcriptional regulation. In the human proximal tubular HK-2 cell line, high glucose increased protein kinase B (AKT) phosphorylation, peroxisome proliferator-activated receptor γ (PPARγ) expression, and CD36 mRNA and protein. Pharmacological inhibition of this pathway reduced CD36 expression and lipid deposition; PPARγ agonism and antagonism produced opposing effects on CD36 abundance. CD36 silencing with small interfering RNA (siRNA) also reduced lipid accumulation, supporting a functional role for CD36 in glucose-induced lipid accumulation in HK-2 cells [24].

A podocyte study identified a regulatory mechanism involving dedicator of cytokinesis 5 (*Dock5*), YTH domain family protein 2 (YTHDF2), and liver X receptor α (LXRα). *Dock5* interacted with YTHDF2 and protected this RNA-binding protein from ubiquitination-associated proteasomal degradation. YTHDF2 promoted N^6-methyladenosine (m^6A)-dependent decay of LXRα mRNA; *Dock5* loss destabilized YTHDF2 and thereby increased LXRα abundance. Mutating the m^6A-binding residues of YTHDF2 and targeted demethylation of LXRα transcripts supported the RNA-dependent step. LXRα then activated CD36 transcription. Chromatin immunoprecipitation supported LXRα occupancy at the CD36 promoter, whereas promoter-reporter experiments supported transcriptional activation in podocytes. The identified m^6A-dependent step acts on upstream LXRα mRNA, linking RNA turnover to CD36 transcription [16].

These studies identify distinct mechanisms regulating CD36 in tubular cells and podocytes: glucose-responsive transcriptional signaling and turnover of an upstream regulatory transcript [16,24].

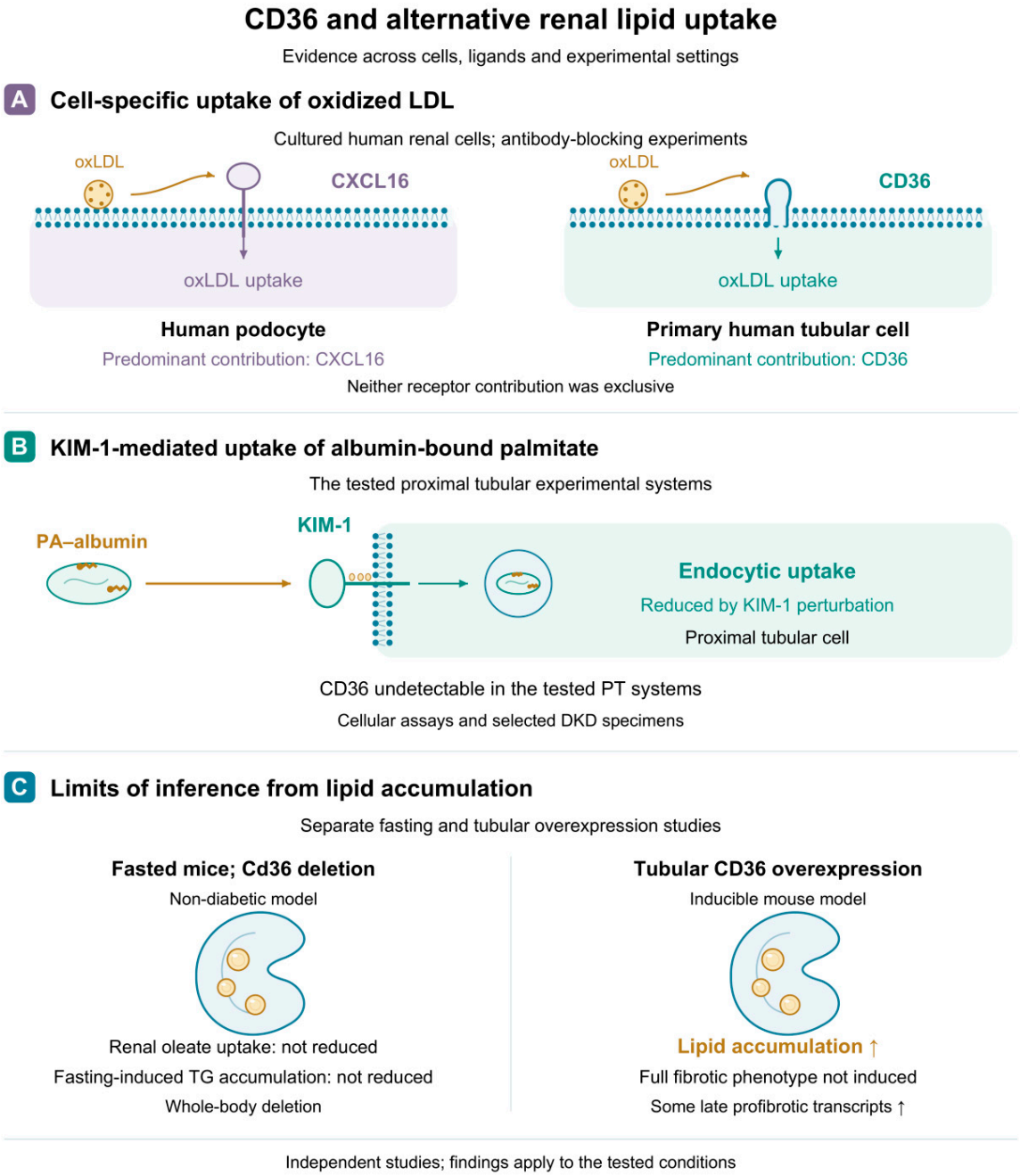


Figure 2. CD36 and alternative pathways of renal lipid uptake across experimental settings. (**A**) Antibody-blocking experiments in cultured human renal cells identified a predominant contribution of CXCL16 to oxLDL uptake in podocytes and of CD36 in primary tubular cells; neither contribution was exclusive [21]. (**B**) KIM-1 mediated endocytic uptake of albumin-bound palmitate. KIM-1 knockdown or mucin-domain disruption reduced uptake. CD36 was undetectable in KIM-1-expressing LLC-PK1 cells, primary mouse proximal tubular cells, and the DKD proximal tubules examined in that study [22]. (**C**) In a non-diabetic fasting model, global *Cd36* deletion did not reduce renal oleate uptake or fasting-induced triglyceride accumulation; systemic fatty acid exposure also differed [5]. In a separate tubular CD36-overexpression model, increased lipid accumulation was insufficient for a full fibrotic phenotype, although some profibrotic transcripts increased modestly at a later time point [23]. Arrows summarize functional uptake relationships within each study. The findings apply to the tested conditions, and particle counts are schematic. No compensatory receptor induction or receptor competition is proposed. CXCL16, C-X-C motif chemokine ligand 16; KIM-1, kidney injury molecule-1; oxLDL, oxidized low-density lipoprotein; PA, palmitic acid; PT, proximal tubule; TG, triglyceride.

2.3. Post-Translational Regulation: Palmitoylation, Trafficking, and Degradation

CD36 function also depends on the amount of receptor present at the plasma membrane. In conditionally immortalized human podocytes, high glucose reduced APT1 expression and its association with CD36, while increasing CD36 palmitoylation and membrane-associated abundance. APT1 overexpression reduced both CD36 palmitoylation and membrane abundance. It also shifted CD36 localization from Rab11-associated recycling compartments toward compartments associated with Rab7 or lysosome-associated membrane protein 1 (LAMP1), accompanied by increased ubiquitination. These results are consistent with altered endosomal sorting and lysosomal degradation, although compartmental colocalization alone does not measure trafficking kinetics [17].

Site-directed experiments strengthened the connection between palmitoylation and receptor function. Among the tested CD36 cysteine substitutions, C466S markedly reduced palmitoylation and membrane-associated abundance in site-directed assays. In a separate experiment, after lentiviral short hairpin RNA (shRNA) depletion of endogenous CD36, C466S reconstitution produced less lipid accumulation and apoptosis than wild-type CD36 reconstitution under high glucose. APT1 reduced these outcomes in the wild-type group. The APT1 inhibitor ML348 partly counteracted APT1 overexpression in additional experiments. These site-directed and reconstitution findings connect Cys466-dependent receptor regulation with membrane-associated CD36 and the lipid-loading and apoptotic responses of high-glucose-exposed podocytes [17].

Surface CD36 can also respond differently to genetic and pharmacological manipulation of the same upstream protein. In a non-DKD, high-fat-diet model, deletion of the gene encoding proprotein convertase subtilisin/kexin type 9 (PCSK9) increased renal CD36 and lipid accumulation, whereas inhibitory PCSK9 antibodies reduced surface CD36 and renal lipid-associated injury. The investigators proposed that antibody-bound PCSK9 retained the ability to promote CD36 degradation despite inhibiting its interaction with LDL receptors. This non-diabetic comparison shows why the direction of a genetic phenotype may not predict the effect of an antibody that changes only selected protein interactions [25]. Figure 3 contrasts the transcriptional and post-translational mechanisms established in podocyte models.

2.4. NRF2: Antioxidant Defense and Metabolic Regulation Can Diverge

Studies of nuclear factor erythroid 2-related factor 2 (NRF2) show that its effects on antioxidant defense and kidney injury do not always coincide. In db/db mice, global *Nrf2* deficiency reduced renal proximal tubular CD36 and fatty acid-binding protein 4 (FABP4) expression, lipid accumulation, albuminuria, and selected injury measures. Blood glucose and blood pressure also fell. Dihydroethidium (DHE) and 8-hydroxy-2′-deoxyguanosine staining remained elevated relative to non-diabetic controls, with no significant difference reported between the two diabetic genotypes. Thus, improvement in selected renal phenotypes did not require a detectable reduction in these markers of oxidative stress. NRF2-deficient HK-2 cells also showed reduced CD36 expression and altered responses to NRF2 activation and fatty acid exposure [26].

Systemic changes in glycemia and blood pressure limit attribution to a local NRF2–CD36 mechanism. The study also lacked CD36-specific rescue and direct testing of NRF2 occupancy at the tubular CD36 promoter. Lipid accumulation was lower in diabetic *Nrf2*-deficient mice, whereas DHE and 8-hydroxy-2′-deoxyguanosine staining did not differ significantly between the diabetic genotypes [26].

An opposing renal phenotype was reported in insulin-deficient Akita mice. Global *Nrf2* deficiency aggravated oxidative injury and kidney damage, whereas partial knockdown of Kelch-like ECH-associated protein 1 (*Keap1*), which modestly activates NRF2, attenuated

tubulointerstitial injury. CD36 dependence was not examined [27]. Differences in diabetic background, systemic metabolism, intervention direction, and disease duration complicate direct comparison with the db/db findings. Taken together, these studies support assessing antioxidant capacity, lipid handling, and systemic metabolic responses together when evaluating NRF2 modulation (Table 1).

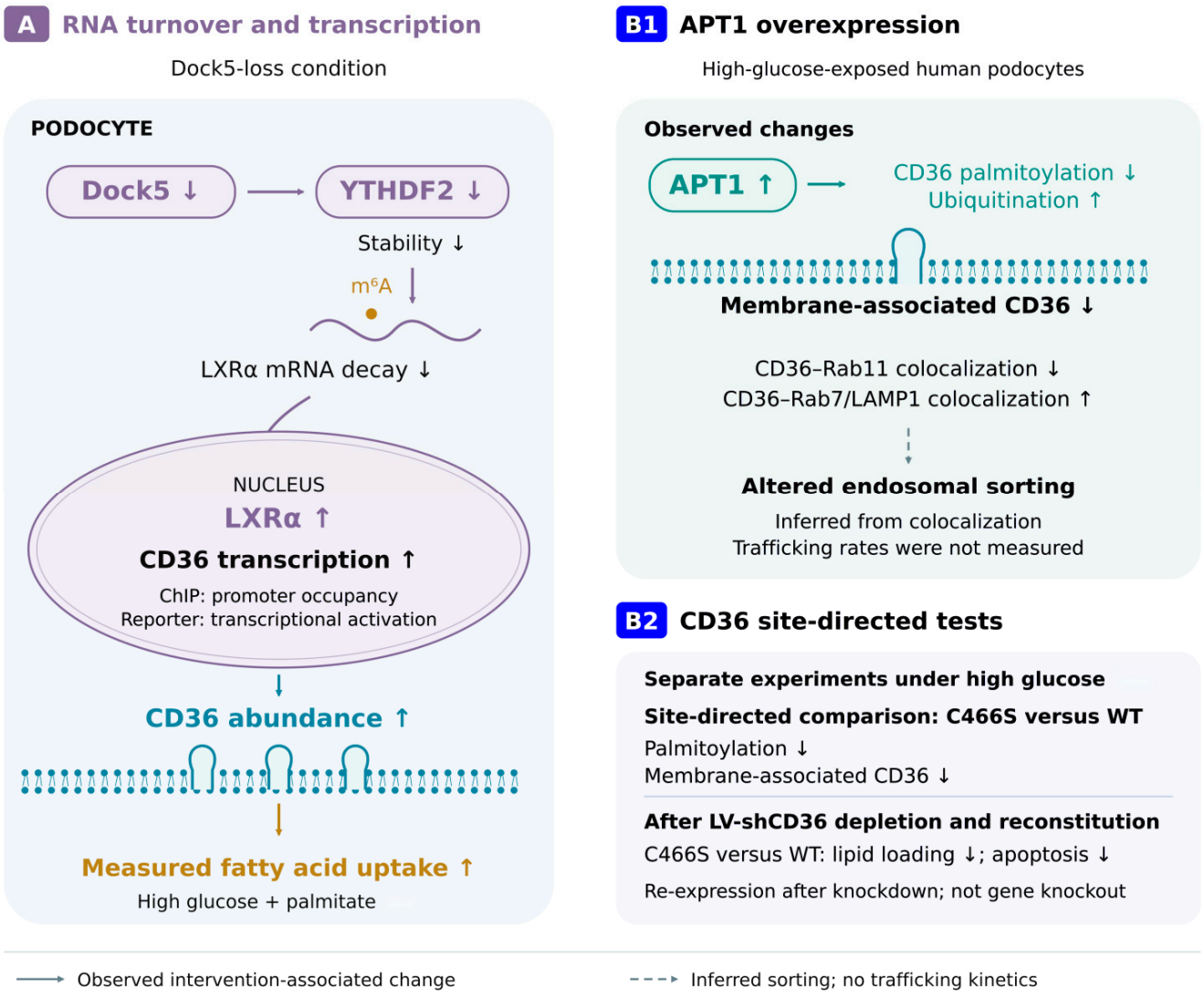


Figure 3. Mechanisms regulating CD36 availability in podocyte models. (**A**) *Dock5* loss destabilizes YTHDF2, reducing m^{6}A-dependent decay of upstream LXRα mRNA and increasing LXRα-dependent CD36 transcription and measured fatty acid uptake. Chromatin immunoprecipitation supported promoter occupancy; reporter experiments supported transcriptional activation [16]. (**B1**) APT1 overexpression in high-glucose-exposed human podocytes reduced CD36 palmitoylation and membrane-associated abundance, increased ubiquitination, and altered compartmental colocalization. Dashed arrows indicate sorting inferred from colocalization, without measurement of trafficking kinetics. (**B2**) Site-directed comparisons assessed palmitoylation and membrane-associated CD36. In separate experiments after lentiviral shRNA-mediated CD36 knockdown, C466S reconstitution produced less lipid loading and apoptosis than WT reconstitution [17]. Solid arrows indicate observed intervention-associated changes. These experiments do not establish a podocyte-specific in vivo CD36 rescue. APT1, acyl-protein thioesterase 1; CD36, cluster of differentiation 36; *Dock5*, dedicator of cytokinesis 5; LAMP1, lysosome-associated membrane protein 1; LXRα, liver X receptor α; m^{6}A, N^6-methyladenosine; shRNA, short hairpin RNA; WT, wild type; YTHDF2, YTH domain family protein 2.

Table 1. Contrasting NRF2-related findings and their relevance to CD36 research.

Study and Setting	Perturbation or Treatment	Principal Observation	Interpretation for CD36 Targeting
Su et al. (2023) [26]; db/db mice; HK-2 cells	Global *Nrf2* deficiency; cellular NRF2 deletion	Lower tubular CD36, lipid accumulation, and selected measures of renal injury; no significant difference in DHE/8-OHdG staining between diabetic genotypes. Glucose and blood pressure also fell.	Neither CD36-specific rescue nor direct renal promoter occupancy was established.
Liu et al. (2022) [27]; insulin-deficient Akita mice	Global *Nrf2* loss; partial *Keap1* knockdown	*Nrf2* loss worsened oxidative injury and kidney damage; modest NRF2 activation attenuated tubulointerstitial injury.	CD36 dependence was not tested; diabetic backgrounds and systemic effects differ.
de Zeeuw et al. (2013) [28]; BEACON; T2D with stage 4 CKD	Bardoxolone methyl versus placebo	Higher eGFR coexisted with more heart-failure events; the primary renal/cardiovascular composite was not improved.	A clinical endpoint and safety comparison, not a trial of CD36-directed treatment.

These studies address different interventions and outcomes. Their juxtaposition does not establish a shared CD36 mechanism or a uniform effect of NRF2 modulation. Abbreviations: CD36, cluster of differentiation 36; CKD, chronic kidney disease; DHE, dihydroethidium; eGFR, estimated glomerular filtration rate; HK-2, human proximal tubular cell line; *Keap1*, Kelch-like ECH-associated protein 1; NRF2, nuclear factor erythroid 2-related factor 2; T2D, type 2 diabetes; 8-OHdG, 8-hydroxy-2′-deoxyguanosine.

3. CD36-Associated Lipotoxic Injury in Renal Cells

Studies in renal cells examine both ligand handling and responses to metabolic stress. Measuring uptake, substrate utilization, signaling, and injury in the same experimental system is essential to identifying the processes affected by CD36.

3.1. Proximal Tubular Epithelial Cells

3.1.1. Substrate Handling and Mitochondrial Metabolism

The uptake studies discussed in Section 2.1 identify CD36-dependent responses to particular ligands and alternative routes for albumin-bound fatty acids. Another question is whether CD36 affects the ability of tubular cells to metabolize incoming lipids. In diabetic mice, global *Cd36* deletion reduced renal injury, extracellular matrix accumulation, and apoptosis and improved tubular mitochondrial morphology. Primary tubular cells isolated from these animals showed improved oxygen consumption and adenosine triphosphate (ATP)-related measurements, while renal peroxisome proliferator-activated receptor α (PPARα) and fatty acid oxidation (FAO)-associated expression recovered. The investigators proposed involvement of pyruvate dehydrogenase kinase 4 (PDK4) and AMP-activated protein kinase (AMPK). However, blood glucose was substantially lower in the diabetic knockout animals, leaving systemic metabolic improvement as a contributor to the renal phenotype [6].

Cell experiments conducted at a fixed extracellular glucose concentration help distinguish changes in cellular CD36 function from the effects of lower blood glucose. In HK-2 cells, CD36 knockdown increased palmitate-dependent oxygen consumption, restored AMPK phosphorylation and FAO-associated proteins, and reduced the shift toward glycolytic metabolism [29]. Uptake, lipid partitioning, and mitochondrial substrate use represent distinct processes, so lipid droplets or gene expression alone provide an incomplete metabolic account. Considered alongside the knockout findings, these cell experiments

support impaired oxidative substrate use as a functional component of CD36-associated tubular injury [6,29].

3.1.2. Oxidant Signaling, Inflammation, and Apoptosis

Mitochondrial oxidants provide an experimentally supported link between metabolic dysfunction and inflammation. In high-glucose-treated HK-2 cells, CD36 knockdown reduced the mitochondrial oxidant-probe signal, markers of NLR family pyrin domain-containing 3 (NLRP3) inflammasome activation, and interleukin-1β (IL-1β) secretion. CD36 overexpression strengthened the inflammatory response, which the mitochondria-targeted antioxidant mitoTEMPO attenuated. In db/db mice, systemically administered CD36 shRNA lentiviral vectors also reduced tubular injury, inflammatory infiltration, and apoptosis. Blood glucose also decreased after systemic CD36 silencing, so improved glycemia may have contributed to the renal benefit. The controlled cell perturbation and antioxidant experiments more directly connect CD36 to mitochondrial oxidant signaling and inflammatory amplification [29].

Ligand-triggered signaling offers a complementary explanation for tubular injury. In the early study by Susztak and colleagues, high glucose increased surface CD36 and sensitized cultured tubular cells to glycated albumin and palmitate. Receptor blockade and recombinant-expression experiments implicated sequential Src, p38 mitogen-activated protein kinase, and caspase-3 activation in apoptosis. Proximal tubular CD36 was scarce in the diabetic mouse models examined, but expression of recombinant CD36 rendered otherwise resistant mouse tubular cells susceptible to glycated albumin [19]. Thus, receptor availability can determine the response to a ligand even when increased intracellular lipid storage has not been established as the intervening cause.

Advanced oxidation protein products (AOPPs) extend this ligand repertoire. A study of cultured proximal tubular cells, non-diabetic uninephrectomized rats and mice, and IgA-nephropathy biopsy tissue linked AOPP exposure to activation of the intrarenal renin–angiotensin system. Cellular CD36 silencing attenuated protein kinase Cα phosphorylation, NADPH oxidase activation, and oxidant production; adding blockade of the receptor for advanced glycation end products produced greater attenuation [30]. In a subsequent study, the indexed abstract reports AOPP-associated lipotoxicity in high-glucose-exposed HK-2 cells, attenuation by CD36 inhibition, and β-catenin-associated regulation of the CD36 promoter [31]. These findings suggest that AOPPs may amplify injury under diabetic metabolic stress; the interpretation is limited to the findings reported in the indexed abstract.

Autophagy-related measurements provide another perspective on the cellular treatment response. Colquhounia root tablet treatment reduced CD36 expression and apoptosis in streptozotocin (STZ)-induced diabetic rats and glucose-stressed HK-2 cells, alongside higher AMPK phosphorylation and altered microtubule-associated protein 1 light chain 3 (LC3), sequestosome 1 (p62), Beclin-1, and autophagosome measurements. Static autophagy markers describe autophagosome abundance; dynamic flux measurements and direct AMPK perturbation would clarify the proposed AMPK–autophagy contribution. CD36 overexpression weakened the cellular protection, providing functional support for receptor involvement in the treatment response [32].

3.1.3. Fibrosis-Associated Responses and Their Experimental Boundaries

The distinction between substrate loading and damage is especially clear in fibrosis experiments. Kang and colleagues analyzed 95 microdissected human kidney tubule samples, including diabetic and hypertensive CKD, and linked fibrotic disease with reduced FAO-related expression. In their Pax8rtTA/TRE-CD36 model, tubular CD36 overexpression produced lipid accumulation without a full fibrotic phenotype: early fibrosis and

apoptosis readouts were unchanged, later profibrotic transcript changes were modest, and susceptibility to STZ-induced diabetic injury was not increased. Genetic or pharmacological improvement of FAO protected against experimental fibrosis [23]. These findings support deficient substrate utilization as a contributor to injury and show that CD36-associated lipid storage alone is insufficient to explain all fibrotic outcomes. The mixed CKD cohort and the predominance of non-DKD fibrosis models limit direct extrapolation to diabetic kidney disease.

CD36 deficiency nevertheless reduced collagen accumulation and nuclear factor κB (NF-κB) activation in hypercholesterolemic mice subjected to unilateral ureteral obstruction. At day 7, renal hydroxyoctadecadienoic acid (HODE) and protein carbonyl content were lower, providing biochemical evidence of reduced lipid and protein oxidation. The F4/80-positive interstitial area was greater in knockout mice despite less fibrosis [33]. This divergence cautions against interpreting macrophage-associated staining as a proxy for profibrotic activity. Whole-body deletion and the obstructive model do not establish a tubular cell-specific mechanism in DKD.

Other studies have examined the contribution of CD36 to profibrotic signaling. In sodium-oleate-exposed rat renal epithelial NRK-52e cells, CD36 silencing altered the response to Mori Cortex phenolic compounds assessed through transforming growth factor-β (TGF-β), zinc finger E-box-binding homeobox 1 (ZEB1), and Snail1 [34]. In TGF-β-treated HK-2 cells, CD36 knockdown and overexpression changed fibrosis-associated markers in a fisetin study [35]. These non-diabetic culture systems characterize epithelial signaling responses rather than lineage conversion into matrix-producing interstitial cells or progressive fibrosis. Together, the experiments link CD36 perturbation to epithelial profibrotic responses across distinct lipid and cytokine challenges [34,35].

3.2. Podocytes

3.2.1. Membrane Availability, Lipid Uptake, and Structural Injury

Evidence linking CD36 to podocyte lipotoxicity initially combined diabetic human tissue with a palmitate-exposed cell model. Hua and colleagues reported increased renal CD36 staining in 20 patients with diabetic nephropathy and hyperlipidemia compared with 18 controls. In cultured mouse podocytes, palmitate increased CD36 expression and membrane localization, lipid accumulation, reactive oxygen species, and apoptosis. Sulfo-N-succinimidyl oleate (SSO), used to inhibit CD36-associated fatty acid uptake, attenuated lipid accumulation, oxidative stress, and apoptosis. Tempol also reduced palmitate-induced oxidative stress and apoptosis, supporting an oxidative component of the injury. The human findings establish an association, while the functional evidence comes predominantly from pharmacological experiments in culture [20].

The *Dock5* study combined fluorescent and labeled-palmitate uptake assays with measurements of cytotoxicity, mitochondrial oxidative stress, respiration, and actin remodeling. Under high-glucose and palmitate conditions, *Dock5* silencing increased uptake and injury, while the measured de novo fatty acid synthesis and oxidation were not significantly altered. SSO attenuated the excess uptake and several injury endpoints [16]. These results identify increased uptake as the detected metabolic change and show that the response is sensitive to SSO; inhibitor specificity is assessed in Section 6.1.

Podocyte-specific *Dock5* deletion aggravated albuminuria, glomerular pathology, basement membrane thickening, foot process effacement, and podocyte loss in mice exposed to a high-fat diet and STZ, without a corresponding change in blood glucose. Podocyte-directed LXRα interference attenuated several effects of *Dock5* loss, and renal adenoviral Dock5 restoration reduced lipid accumulation and structural injury [16]. These interventions establish a role for podocyte *Dock5*–LXRα signaling in this diabetic model; CD36 was

tested pharmacologically in culture. The study also included separate experiments in focal segmental glomerulosclerosis.

APT1 experiments examined how post-translational regulation affects receptor function. The C466S experiments described in Section 2.3 link a receptor variant to lower membrane-associated abundance and, in a separate reconstitution experiment, to less lipid accumulation and apoptosis under the same high-glucose exposure. In db/db mice, intrarenal administration of an adeno-associated virus serotype 9 vector with a cytomegalovirus promoter (AAV9-CMV) expressing APT1 at 16 weeks was followed by assessment at 22 weeks, with five animals per group. Treatment reduced glomerular palmitoylated and membrane-associated CD36, lipid accumulation, and foot process abnormalities; supplementary analyses reported lower urine albumin-to-creatinine ratio (UACR) and serum creatinine. Serum triglycerides and cholesterol also declined [17].

Together, the *Dock5* and APT1 studies delineate complementary transcriptional and post-translational routes regulating CD36 availability in podocytes [16,17]. *Dock5* manipulation links an upstream pathway to diabetic podocyte injury in vivo, while CD36 reconstitution links the C466S receptor variant to reduced lipid loading and apoptosis in culture.

3.2.2. Complementary Mechanisms in Non-DKD Podocyte Models

Experiments in palmitate-exposed podocytes link lipid-induced injury to organelle stress. SSO, the mitochondrial antioxidant mitoTEMPO, and phospholipase C inhibition each attenuated components of an endoplasmic reticulum (ER) calcium-depletion response [36]. A study in high-fat-fed rats and lipid-stressed podocytes linked CD36-related lipid loading to oxidative stress and cytoskeletal disruption, with SSO providing protection in the cell experiments [37]. These models extend the observed injury phenotype to ER calcium regulation and podocyte structure.

In an obesity-related glomerulopathy study, CD36 siRNA or SSO attenuated leptin-induced podocyte injury and NLRP3-associated responses; NLRP3 inhibition reduced injury without reducing measured lipid deposition [38]. This comparison shows that inflammatory injury can be attenuated despite persisting lipid storage. In a separate adriamycin/nephrotic-syndrome investigation, anti-CD36 treatment reduced LDL/IL-1β-associated lipid accumulation and apoptosis in cultured podocytes [39]. Together, these studies relate receptor-associated lipid handling and inflammatory responses to podocyte injury in distinct non-DKD settings.

Other experiments implicate ligand-induced CD36 signaling in podocyte injury. Thrombospondin-1 (TSP1) induced human podocyte apoptosis through a CD36-associated p38 response in an adriamycin-nephropathy investigation, although the in vivo deletion targeted TSP1 [40]. An obesity study combined global *Tsp1* or *Cd36* deficiency with a peptide interrupting TSP1–CD36 interaction. The peptide reduced palmitate-associated apoptosis and albumin passage in cultured podocytes, and global loss of either protein reduced markers of apoptosis in high-fat-fed mice [41]. Across these non-DKD models, ligand-triggered signaling provides a complementary route through which CD36 can influence podocyte injury alongside its role in lipid handling [40,41].

3.3. Mesangial Responses to Lipid Exposure

Studies in mesangial cells link CD36 manipulation to calcium-dependent profibrotic responses. In palmitate-exposed human glomerular mesangial cells, CD36 knockdown attenuated increased intracellular calcium and nuclear factor of activated T cells 2 (NFAT2) expression. Interference with transient receptor potential canonical channel 6 (TRPC6) or NFAT2 reduced fibrosis-associated responses. Prolonged palmitate exposure decreased

TRPC6 expression despite pathway activation, separating channel abundance from signaling output [42].

A complementary astragaloside IV study measured fatty acid uptake, lipid accumulation, oxidant-sensitive fluorescence, and matrix-related proteins in human mesangial cells. Astragaloside IV and SSO attenuated selected palmitate-induced responses, without greater protection from their combination; renal CD36 expression also fell in high-fat-diet/STZ diabetic rats [43]. Both mesangial reports were assessed from abstracts and share several authors. The accompanying whole-kidney expression measurement concerns a different level of evidence from the cultured-cell experiments. Together, the culture findings relate CD36-associated lipid handling to calcium-dependent and matrix-associated responses in mesangial cells [42,43].

3.4. Substrate Exposure, Oxidant Production, and Peroxide Defense

Studies in epithelial cells implicate different metabolic processes in CD36-associated injury. Tubular receptor knockdown improved FAO-related function and reduced mitochondrial oxidant signals, whereas *Dock5* silencing in podocytes increased uptake without a significant change in the reported fatty acid synthesis or oxidation assays [16,29]. Uptake and intracellular substrate use therefore need separate interpretation when comparing renal compartments.

Substrate identity further modifies injury. A cultured-podocyte comparison reported CD36 redistribution and lipid accumulation after either palmitate or oleate exposure, but increased oxidant-sensitive fluorescence and mitochondrial damage predominantly after palmitate [44]. Similar receptor redistribution and storage can therefore accompany different injury phenotypes, implicating the metabolic consequences of the lipid challenge.

Relating lipid loading to ferroptosis requires separate assessment of neutral-lipid storage and the composition and oxidation of susceptible membrane phospholipids. In non-DKD systems, acyl-CoA synthetase long-chain family member 4 (ACSL4) altered phospholipid composition and ferroptosis sensitivity [45], while redox lipidomics identified oxidized arachidonoyl- and adrenoyl-containing phosphatidylethanolamines as relevant products [46]. These findings provide a biochemical framework for investigating the susceptible membrane-lipid pool in diabetic renal cells.

Redox-related rescue experiments address different outcomes. mitoTEMPO attenuated CD36-enhanced NLRP3-associated inflammation in HK-2 cells [29]. In primary tubular cells, CD36 silencing reduced lipid-peroxidation measures and cell death, whereas ferrostatin-1 protection was tested separately under high-glucose/palmitate conditions [18]. The ferroptotic interpretation applies to the cultured-cell conditions examined, as detailed in Section 4.2. Together, these culture studies distinguish a mitochondrial oxidant–inflammatory response from lipid-peroxidation-associated cell injury, providing complementary ways to evaluate CD36-related tubular injury (Table 2).

Table 2. Receptor interventions, functional measurements, and rescue in selected renal studies.

Study and System	Receptor Test	Lipid or Membrane Measurement	Redox or Injury Evidence	Interpretation and Limitations
Susztak et al. (2005) [19] Tubular cells	CD36 blockade and recombinant expression	Surface CD36 under high glucose; glycated albumin/palmitate exposure	Src/p38/caspase-associated apoptosis; receptor blockade	Ligand sensitivity depends on receptor availability in cells; tissue staining is associative.

Table 2. *Cont.*

Study and System	Receptor Test	Lipid or Membrane Measurement	Redox or Injury Evidence	Interpretation and Limitations
Hou et al. (2021) [29] HK-2; db/db mice	CD36 knockdown or overexpression; systemic shRNA	Palmitate-dependent respiration, extracellular acidification rate (ECAR), FAO-related proteins	MitoNeoD signal, NLRP3/IL-1β; mitoTEMPO rescue	Links receptor perturbation to metabolism and oxidant signaling; systemic delivery and lower glycemia limit renal attribution.
Niu et al. (2023) [6] Diabetic mice	Global *Cd36* deletion	Renal lipid accumulation; tubular respiration and mitochondrial morphology	Reduced injury and apoptosis; improved measures of mitochondrial function	Whole-body effect; lower glycemia limits attribution to renal CD36.
Hua et al. (2015) [20] Podocyte culture	SSO inhibition	Membrane localization and lipid accumulation	Oxidant-sensitive fluorescence/apoptosis; Tempol protection	SSO-sensitive oxidative injury; inhibitor specificity and receptor genetic rescue require separate assessment.
Qu et al. (2024) [16] Podocytes; HFD/STZ mice	*Dock5*/LXRα manipulation; cellular SSO	Labeled fatty acid uptake; synthesis/oxidation assays; respiration	Mitochondrial oxidative stress and structural injury; SSO attenuation	Podocyte-specific *Dock5* evidence in vivo; cellular SSO rescue does not isolate CD36 from other drug effects.
Wang et al. (2025) [17] Podocytes; db/db mice	APT1 manipulation; site-directed CD36 assays; separate shRNA depletion with WT/C466S reconstitution	Palmitoylation, membrane protein, compartment colocalization, lipid staining	Apoptosis and structural injury; APT1/ML348 interventions	Reconstitution links the variant to lipid loading and apoptosis; site-directed membrane assays are separate. Colocalization does not quantify trafficking. In vivo APT1 delivery was not podocyte-specific CD36 rescue.
Wang et al. (2025) [18] Primary tubular cells	Recipient-cell CD36 siRNA; IL-1β/p65 interventions	Membrane CD36, lipid staining and cellular lipid measurements	Liperfluo, MDA, GSH, GPX4 protein and cell death; Fer-1 protection in a separate HGPA experiment	CD36 contributes to cytokine-amplified injury in vitro; GPX4 activity and oxidized lipid species were not measured. In vivo intervention targeted *Trem2*.
Kang et al. (2015) [23] Tubular overexpression	Inducible tubular human CD36	Lipid accumulation with assessment of FAO-related pathways	No full fibrotic phenotype from receptor overexpression alone	Storage was insufficient for fibrosis in this setting; the finding cannot be generalized to all DKD models.

Measurements and rescue experiments are compared within their original systems; they do not form a single proven sequence across models. APT1, acyl-protein thioesterase 1; CD36, cluster of differentiation 36; DKD, diabetic kidney disease; ECAR, extracellular acidification rate; FAO, fatty acid oxidation; Fer-1, ferrostatin-1; GPX4, glutathione peroxidase 4; GSH, glutathione; *Dock5*, dedicator of cytokinesis 5; HFD/STZ, high-fat diet/streptozotocin; HGPA, high glucose and palmitate; HK-2, human proximal tubular cell line; IL-1β, interleukin-1β; LXRα, liver X receptor α; MDA, malondialdehyde; NLRP3, NLR family pyrin domain-containing 3; shRNA, short hairpin RNA; siRNA, small interfering RNA; SSO, sulfo-N-succinimidyl oleate. WT, wild type.

The specificity of the assays limits how precisely these processes can be identified. The HK-2 study measured mitochondria-targeted MitoNeoD fluorescence and assessed mitochondrial content using MitoTracker Green. CD36 manipulation and mitoTEMPO rescue provided functional context for interpreting the fluorescence signal [29]. Measurement guidance distinguishes probe oxidation, a defined reactive species, and accumulated molecular damage; DHE fluorescence alone does not resolve all oxidation products, and damage-marker abundance also reflects repair and removal [47]. Accordingly, the absence of a significant difference in DHE and 8-hydroxy-2′-deoxyguanosine staining between the diabetic genotypes does not exclude changes in other cellular redox processes [26]. In DKD models, receptor-dependent intervention paired with chemically defined lipid products would more directly connect membrane function to oxidative injury.

4. Immune and Epithelial Communication: Ferroptosis and Profibrotic Signaling

4.1. CD36-Associated Macrophage States

CD36 can couple macrophage cargo recognition to inflammatory signaling. In non-DKD experimental systems, Stewart and colleagues showed that oxidized LDL or amyloid-β recognition initiated assembly of a CD36-dependent Toll-like receptor 4–Toll-like receptor 6 complex [48]. Sheedy and colleagues subsequently connected CD36-mediated oxidized LDL uptake with intracellular cholesterol crystallization, lysosomal destabilization, and NLRP3-dependent IL-1β release [49]. These studies identify experimentally supported mechanisms linking receptor recognition and uptake to inflammatory signaling and lysosomal injury, providing a basis for investigating these processes in diabetic renal macrophages.

Kidney transcriptomic studies identify the cells in which that question can be tested. One integrated analysis placed CD36 among macrophage-associated phagosome or efferocytosis genes and found an inverse association with glomerular filtration rate (GFR). High glucose reduced engulfment of apoptotic tubular cells by RAW264.7 macrophages, but CD36 was not manipulated in that assay [50]. A single-cell analysis of urine-derived cells linked macrophages expressing CD36 transcripts to a transcriptional state related to interleukin-6 (IL-6), Janus kinase (JAK), and signal transducer and activator of transcription 3 (STAT3), and inferred inflammatory or profibrotic communication. Colocalization with the macrophage marker F4/80 was examined separately in animal tissue [51]. In that analysis, CD36 defined the cell subgroup rather than functioning as the modeled ligand or receptor in the inferred interactions. Together, these findings localize CD36-associated macrophage states and prioritize candidate efferocytosis and communication pathways for receptor-directed investigation in DKD.

In a non-diabetic obesity/inflammation model, global *Cd36* deficiency reduced renal lipid deposition and injury, while cellular silencing attenuated cytokine-associated fatty acid accumulation in mesangial and HK-2 cultures [52]. These findings suggest that inflammation modifies CD36-associated lipid handling and support further investigation of the renal immune populations involved in diabetes.

4.2. TREM2 and IL-1β Regulation of Tubular CD36 in Ferroptosis-Associated Injury

A study using *Trem2*-deficient mice and macrophage-conditioned medium tested the role of triggering receptor expressed on myeloid cells 2 (TREM2) in immune–epithelial communication. In a high-fat diet/streptozotocin model incorporating unilateral nephrectomy, *Trem2* loss aggravated tubular lipid accumulation and ferroptosis-associated injury. Under high-glucose/palmitate conditions, *Trem2*-deficient bone marrow-derived macrophages showed enhanced extracellular signal-regulated kinase (ERK) signaling and IL-1β production. Their conditioned medium, applied together with high glucose and palmitate to

primary tubular epithelial cells, increased membrane-associated CD36, lipid accumulation, lipid peroxidation, and cell death. IL-1β neutralization and inhibition of macrophage ERK signaling attenuated these responses [18].

Silencing CD36 in recipient tubular cells reduced lipid accumulation, malondialdehyde and other lipid-peroxidation measures, and cell death, while restoring glutathione levels and glutathione peroxidase 4 (GPX4) protein abundance. Protection was also observed against IL-1β-driven responses. In separate high-glucose/palmitate experiments, ferrostatin-1 protection supported a ferroptotic component [18]. The animal intervention targeted *Trem2*, and no renal cell-specific CD36 rescue was tested in vivo. GPX4 catalytic activity and defined oxidized phospholipid species were not measured. Within the tested primary tubular-cell systems, these complementary experiments support epithelial CD36 as a contributor to cytokine-amplified lipid peroxidation and ferroptosis-associated injury [18].

p65 silencing and pharmacological NF-κB inhibition reduced IL-1β-induced CD36 expression, supporting NF-κB-dependent induction; predicted promoter motifs did not establish direct p65 occupancy. The study also linked *Trem2* loss to impaired clearance of ferroptotic tubular cells, without assigning that macrophage function to CD36 [18]. Figure 4 places the cytokine-amplified epithelial response alongside the distinct mitochondrial oxidant pathway.

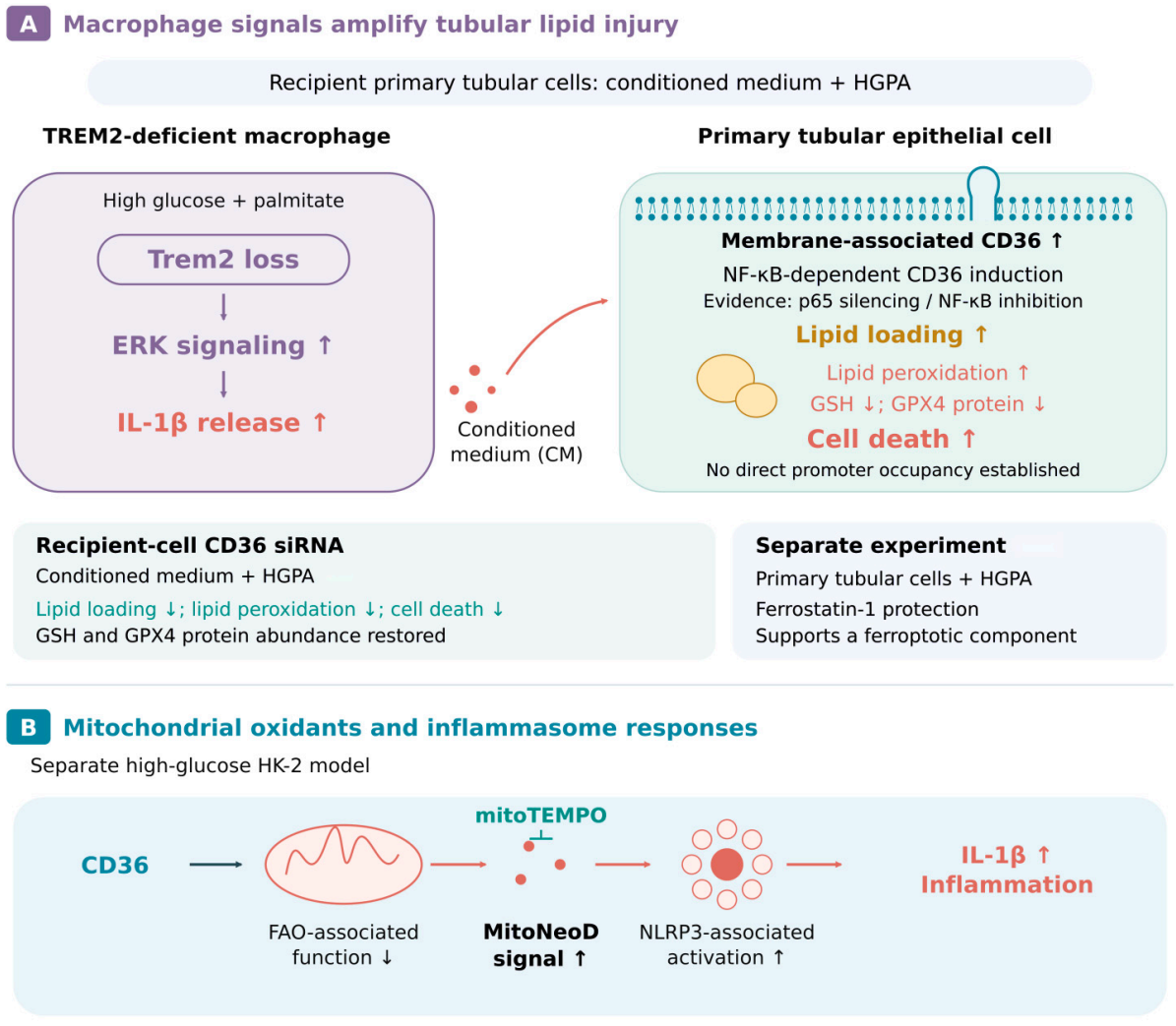


Figure 4. CD36-associated redox injury in distinct tubular experimental systems. (**A**) Under high-glucose/palmitate (HGPA) conditions, *Trem2*-deficient macrophages increase ERK signaling and IL-1β

release. Their conditioned medium was applied together with HGPA to primary tubular epithelial cells. Recipient-cell CD36 silencing attenuated lipid loading, peroxidation and cell death. p65 silencing and NF-κB inhibition supported NF-κB-dependent CD36 induction; direct promoter occupancy was not demonstrated. GPX4 denotes protein abundance, not catalytic activity. Ferrostatin-1 protection was examined in a separate HGPA experiment, supporting a ferroptotic component [18]. These cell experiments do not establish CD36-dependent ferroptosis in vivo. (**B**) In a separate high-glucose HK-2 model, CD36 perturbation was associated with altered FAO-related function, mitochondrial oxidant probe signals (MitoNeoD), and NLRP3-associated inflammation. mitoTEMPO attenuated the inflammatory response [29]. Arrows summarize functional relationships, not direct binding; the blunt line indicates antioxidant intervention. CD36, cluster of differentiation 36; ERK, extracellular signal-regulated kinase; FAO, fatty acid oxidation; GPX4, glutathione peroxidase 4; GSH, glutathione; IL-1β, interleukin-1β; NF-κB, nuclear factor κB; NLRP3, NLR family pyrin domain-containing 3; TREM2, triggering receptor expressed on myeloid cells 2.

4.3. Podocyte-Derived Extracellular Vesicles and Tubular Profibrotic Signaling

In a culture model without a diabetic stimulus, podocyte-derived microparticles increased p38/Smad3 phosphorylation and fibronectin/collagen IV expression in proximal tubular cells; SSO abrogated these responses [53]. This identifies a candidate route of glomerular–tubular communication with an SSO-sensitive profibrotic response (Section 6.1).

A systematic review of preclinical large extracellular vesicles in diabetic nephropathy documents variation in vesicle origin, isolation, characterization, dosing, and endpoints [54]. Testing this pathway in diabetes therefore requires clearly defined vesicle sources and exposure conditions, separate assessment of uptake and signaling, and direct manipulation of CD36 in recipient cells.

5. Human Evidence and Candidate Biomarkers

5.1. Renal Tissue CD36 Expression and Pathological Injury

Herman-Edelstein and colleagues examined renal lipid metabolism in human diabetic nephropathy. They studied archival tissue from 34 patients with diabetic nephropathy (DN) and 12 controls, the latter comprising six living-donor biopsies and six nonaffected nephrectomy regions; some control participants had diabetes without renal involvement. Renal CD36 transcripts were increased alongside reduced FAO-related expression and cholesterol-efflux programs. Lipid staining was performed in a subset of frozen DN biopsies, while lipid-droplet-associated protein staining provided a comparison in processed tissue [55]. This observational tissue comparison did not directly measure CD36-dependent substrate flux. Within its sampling context, the coordinated transcript and histological findings support altered renal lipid handling in human diabetic nephropathy.

Other tissue studies place these metabolic findings in specific renal compartments. Susztak and colleagues associated greater proximal tubular CD36 staining with apoptosis and degeneration in diabetic nephropathy [19]. Hua and colleagues reported increased tubular and glomerular expression in diabetic nephropathy with hyperlipidemia, although the human staining lacked podocyte-marker colocalization [20]. The accompanying cell experiments provide functional evidence distinct from the tissue associations; Table 3 records the sample sizes and comparators.

The source of control tissue also affects interpretation. The NRF2 study examined tumor-free renal-carcinoma nephrectomy regions from four patients with diabetes and four without diabetes; enrollment was based on diabetes status rather than an independently defined DKD biopsy cohort [26]. A later energy-metabolism study compared histologically diagnosed diabetic-nephropathy tissue with paracancerous tissue from normoglycemic patients with renal malignancy [56]. These samples can support expression analyses, but

interpretation as a DKD signature requires consideration of biopsy indication, pathology, treatment, and renal function.

Table 3. Human studies of renal, urinary, and circulating CD36.

Study	Participants or Specimens	Measurement and Design	Main Finding	Limitations
Susztak et al. (2005) [19]	10 diabetic nephropathy; 10 controls; 10 FSGS	Renal staining; archived biopsy/nephrectomy material	Greater proximal tubular staining in diabetic nephropathy, associated with tubular injury.	Tubular association; neither prospective prediction nor human causal intervention.
Herman-Edelstein et al. (2014) [55]	34 DN; 12 controls from donor/nephrectomy tissue	Archival renal transcripts and lipid-related staining; frozen DN subset	Higher CD36 transcripts alongside lower FAO- and cholesterol-efflux-related expression.	Expression does not measure CD36-mediated lipid flux; mixed controls included diabetes without renal involvement.
Hua et al. (2015) [20]	20 diabetic nephropathy; 18 controls	Tubular/glomerular staining; controls from renal-trauma nephrectomy	Increased tubular/glomerular CD36 in diabetic nephropathy with hyperlipidemia.	Selected tissue comparison; human staining lacks podocyte-marker colocalization.
Su et al. (2023) [26]	4 with diabetes; 4 without diabetes	Tumor-free renal-carcinoma nephrectomy regions	Higher proximal tubular CD36/FABP4 staining in diabetes.	Diabetes comparison; not an independently defined DKD biopsy cohort.
Jiang et al. (2026) [56]	10 histologically diagnosed diabetic nephropathy; 6 controls	Renal immunohisto-chemistry; controls from normoglycemic renal-malignancy surgery	Higher CD36 expression in the tissue comparison and in the accompanying database analysis.	Additional tissue-expression validation; selected sources of control tissue and no human CD36 intervention.
Zocchio et al. (2025) [57]	127 T1D recruited; 87 RNA samples analyzed	Urinary-sediment mRNA measured at the last visit; retrospective eGFR data	Higher CD36 mRNA in 23 historical decliners versus 64 nondecliners ($p = 0.016$).	Association with historical decline; baseline CD36 was not tested prospectively.
Shiju et al. (2015) [58]	80; four groups of 20	Plasma and urinary sCD36; in-house ELISA; cross-sectional groups	Higher sCD36 in diabetic microalbuminuria and macroalbuminuria groups.	Association across groups reported in the abstract; no prospective prognostic test.
Moovendhan et al. (2025) [59]	160; four groups of 40	Serum sCD36; case–control comparison across albuminuria categories	sCD36 rose across albuminuria groups; within-cohort AUC 0.908.	Within-cohort discrimination; progression prediction and assay transferability unestablished.

Table 3. *Cont.*

Study	Participants or Specimens	Measurement and Design	Main Finding	Limitations
Wang et al. (2018) [60]	161 CKD; 87 with diabetes and 74 without diabetes	Serum sCD36; hospitalized CKD comparison	Lower sCD36 with diabetes; positive eGFR correlation; group difference nonsignificant after stage stratification.	Mixed CKD etiologies; direction differs from albuminuria-category studies.
Li et al. (2025) [61]	191 T2D with early DKD; 12 weeks	Serum sCD36; control, insulin, and GLP-1RA groups	GLP-1RA treatment was associated with larger decreases in sCD36 and UACR.	Allocation reporting and change-value statistics are inconsistent; baseline imbalances and short follow-up limit causal inference.
González-Luis et al. (2026) [62]	362 T2D with CKD G3a/G3b	Peripheral leukocyte CD36 mRNA	Association with albuminuria; adjusted atherosclerosis association and mediation were nonsignificant.	Systemic cellular expression; renal origin was not established; adjusted association with prevalent subclinical atherosclerosis was nonsignificant.

Study designs and analytes are heterogeneous; these findings should not be pooled as measurements of one renal biomarker. AUC, area under the receiver operating characteristic curve; CD36, cluster of differentiation 36; CKD, chronic kidney disease; DKD, diabetic kidney disease; DN, diabetic nephropathy; eGFR, estimated glomerular filtration rate; ELISA, enzyme-linked immunosorbent assay; FABP4, fatty acid-binding protein 4; FAO, fatty acid oxidation; FSGS, focal segmental glomerulosclerosis; GLP-1RA, glucagon-like peptide-1 receptor agonist; sCD36, soluble CD36 (the conventional assay designation; molecular forms may differ); T1D/T2D, type 1/type 2 diabetes; UACR, urine albumin-to-creatinine ratio.

5.2. Urinary and Circulating CD36 Measurements

Urinary sediment offers a less invasive source for gene-expression analysis. A study recruited 127 individuals with type 1 diabetes, of whom 87 had urinary sediment RNA suitable for analysis. CD36 mRNA was higher in 23 participants classified as renal function decliners than in 64 nondecliners ($p = 0.016$). The difference across the cohort median albumin-to-creatinine ratio of 11 mg/g did not reach conventional statistical significance ($p = 0.051$). Expression correlated with *IL1B* and *TGFB1* and with circulating lipid measures [57]. Sampling at the last evaluation was combined with retrospective clinical records, including a median historical follow-up of 13 years. This design relates current expression to previously documented estimated GFR (eGFR) decline. The findings thus associate urinary-sediment CD36 expression with the history of renal decline and lipid/inflammatory profiles in this type 1 diabetes cohort [57].

Interpretation also depends on the mixture of shed cells in the sediment and the exclusion of samples with inadequate RNA quality. Without cell-specific attribution, changes could reflect altered cellular composition, altered expression within cells, or both. Validation in type 2 diabetes is needed before extending this type 1 diabetes finding to the main clinical population considered here.

Earlier fluid-based evidence came from a study of 80 participants in four groups of 20: normal glucose tolerance and T2D with normoalbuminuria, microalbuminuria, or macroalbuminuria. An in-house sandwich enzyme-linked immunosorbent assay (ELISA) detected higher plasma and urinary soluble CD36 (sCD36) in the albuminuric groups [58]. The

comparison establishes an association across existing categories; a prognostic interpretation would require sampling before subsequent decline. Urinary protein immunoreactivity also differs from the urinary-cell transcript measurement discussed above.

A later case–control study included 160 participants in four groups of 40: healthy controls and participants with diabetes and normoalbuminuria, microalbuminuria, or macroalbuminuria. Serum sCD36 increased across these categories and correlated with glycemic measures, albuminuria, and lower eGFR. A within-cohort receiver operating characteristic analysis reported an area under the curve of 0.908 [59]. Despite the paper's reference to clinical progression, participants were compared across existing disease categories. The study therefore supports cross-sectional discrimination, rather than temporal prediction of progression; its threshold requires independent validation.

The direction of association is not consistent across populations. Wang and colleagues studied 161 hospitalized patients with CKD, including 87 with diabetes and 74 without diabetes. Serum sCD36 was lower in the diabetes group, and correlated positively with eGFR within that group. The between-group difference was no longer significant after stratification by CKD stage [60]. This cohort compared CKD with and without diabetes rather than healthy controls and diabetic albuminuria categories. The finding limits a universal interpretation of higher circulating CD36 as more advanced kidney injury and highlights the influence of comparator selection, disease stage, and assay characteristics.

A single-center study of 191 patients with T2D and early DKD compared control, insulin, and glucagon-like peptide-1 (GLP-1) receptor agonist groups over 12 weeks. The GLP-1 receptor agonist group showed larger reductions in sCD36 and UACR. The authors describe an observational cohort, while also reporting computer-generated block allocation and grouping by treatment regimen. This inconsistent description prevents confident interpretation as a conventional randomized trial. Baseline differences in age, sex, glycemic control, and eGFR further limit causal inference despite the reported adjustments. The authors also reported an association between changes in sCD36 and UACR, but the change-value regression gives a confidence interval crossing the null and a Wald statistic inconsistent with its *p*-value. Consequently, that association cannot be confirmed from the published statistics, and mediation of renal benefit remains unproven [61].

In 362 participants with T2D and moderate CKD, peripheral leukocyte CD36 mRNA was associated with albuminuria and was higher in macroalbuminuria. Its association with subclinical atherosclerosis was not significant in multivariable models, and CD36 was not a significant mediator in the exploratory analyses [62]. Leukocyte expression may inform investigation of systemic inflammatory states and represents a different analyte from soluble protein concentration. The study did not establish an independent association between CD36 expression and prevalent subclinical atherosclerosis [62].

The wider sCD36 literature includes associations across obesity, liver disease, diabetes, and vascular disease and discusses multiple possible cellular sources [63]. The renal specificity of circulating CD36 therefore requires direct validation. Interpretation should account for metabolic and inflammatory comorbidities and establish the cellular source and molecular form detected by the assay before inferring a renal contribution.

5.3. Assay Comparability and Limitations of Clinical Evidence

The term sCD36 also requires an operational definition. In a study of obese people with T2D and lean or obese controls, flow cytometry detected CD36-bearing plasma microparticles with different cellular-marker profiles. Erythrocyte-associated particles accounted for the largest identified fraction in the T2D group, whereas endothelial-associated particles predominated in controls. Particle counts and ELISA-based CD36 protein concentrations were related but differed in their association with diabetes [64]. This was a diabetes biomarker

study, without validation of renal origin or DKD prognosis. It shows why CD36 immunoreactivity should not automatically be interpreted as a freely soluble, kidney-derived receptor fragment. Assay validation should establish which molecular forms are detected and how sample processing affects their recovery.

Renal tissue CD36 expression measurements [19,55,56], urinary-cell and leukocyte mRNA [57,62], and plasma, serum or urinary CD36 immunoreactivity [58–61,64] represent distinct compartments and analytes. Differences in diabetes type, CKD stage, comparator selection and assay design may contribute to opposing associations, but their individual effects have not been isolated. Concentrations and thresholds should not be pooled without harmonized calibration, dilution and sample handling. Serum concentrations differed substantially between two studies despite use of the same units [59,61]. Some group values in one study exceeded the stated assay range [59]; reporting the dilution and back-calculation details would facilitate comparison. These findings support context-specific biomarker hypotheses.

The human studies identify candidate markers of metabolic and inflammatory disease states and support distinct questions for clinical validation: discrimination between existing disease categories, prognosis of renal decline, and monitoring of treatment-associated change. Section 7.3 specifies how prespecified assays, independent cohorts and prospective outcomes can evaluate each intended use.

5.4. Transcriptomic Signatures and Independence of Validation

Archived expression studies have prioritized CD36 in analyses of energy metabolism, copper-related processes, glomerular injury, immune/oxidative stress, and liver–kidney signatures [56,65–68]. One study integrated glomerular and tubular datasets and included human immunohistochemistry [56]. Another combined two glomerular datasets for discovery and evaluated GSE96804 as an external dataset [66]. A separate analysis used GSE104948 for expression and receiver operating characteristic (ROC) validation and GSE131882 for single-nucleus localization [67]. The accessible abstract for a ferroptosis-oriented study reports validation in an independent clinical transcriptomic database and diabetic mice, but does not specify dataset accessions, renal compartments, or participant overlap [69]. Together, these expression-based studies prioritize CD36 across complementary biological programs and identify datasets and renal cell populations for subsequent functional and clinical evaluation.

Supplementary Table S2 specifies each dataset's role and renal compartment and distinguishes within-study validation from cross-publication cohort reuse. One study used discovery SuperSeries GSE30122, which includes the reported validation SubSeries GSE30528 and GSE30529 [65]. The reported sample-exclusion details do not confirm whether the validation data were independent of discovery. Another cross-disease analysis used DN data in shared-gene selection before model assessment [68]. Cross-publication reuse of a discovery dataset is recorded separately from a study's own external-validation design, which is assessed from its reported data partition. Accession differences alone do not establish donor independence. Prespecified evaluation in independent human cohorts will strengthen assessment of the clinical relevance of these expression findings.

6. Therapeutic Targeting: Receptor Dependence and Redox Consequences

6.1. Genetic Manipulation and Direct Pharmacological Inhibition of CD36

Direct receptor manipulation provides a rationale for therapeutic investigation. Whole-body *Cd36* deletion and systemic lentiviral silencing improved experimental renal outcomes, but both interventions also lowered blood glucose. Their renal effects therefore cannot be separated from improved systemic metabolism without further controls [6,29]. Cellu-

lar SSO experiments complement these results, including rescue after *Dock5* loss [16,20]. How confidently these effects can be attributed to CD36 depends on the specificity of each intervention.

SSO illustrates why binding and functional specificity need separate assessment. Mass spectrometry identified covalent modification of CD36 Lys164. In Chinese hamster ovary cells, the K164A variant failed to enhance labeled palmitate uptake or fatty acid-induced intracellular calcium release, despite total and surface receptor levels similar to those of wild-type CD36 [70]. This comparison supports a functional role for the residue beyond receptor abundance. Experiments in adipocytes, engineered cells, and protein-free vesicles subsequently found that SSO could cross membranes and modify additional proteins; they also separated rapid fatty acid translocation from subsequent metabolism [71]. Together, these studies show that SSO binds CD36 but that sensitivity to SSO does not by itself establish CD36-specific transport. Evidence for a renal CD36 effect is stronger when pharmacological inhibition agrees with genetic loss and rescue at matched receptor expression levels under the same uptake conditions.

The 5A apolipoprotein A-I mimetic peptide study offers a useful design for that comparison. In a non-DKD model using subtotal nephrectomy and angiotensin II infusion, global *Cd36* deletion and 5A treatment each reduced functional and histological deterioration without a corresponding blood-pressure reduction. Addition of 5A to *Cd36*-deficient mice produced no further renal improvement. A separate ureteral-obstruction experiment also showed less fibrosis [72]. The absence of an additional drug effect does not establish exclusive molecular targeting. Together with ligand-competition assays, however, the genetic–pharmacological comparison provides functional evidence of a CD36-dependent effect and a practical template for evaluating receptor dependence in diabetic renal models.

6.2. Upstream Regulators and Pharmacological Modulation

In high-glucose-exposed podocytes, APT1 overexpression increased CD36 ubiquitination and reduced membrane-associated CD36; separate WT/C466S reconstitution experiments linked the variant to reduced lipid loading and apoptosis [17]. In tubular cells, APT1-mediated depalmitoylation of β-catenin at Cys300 reduced its ubiquitination and increased its stability. Tubular *Apt1* deletion or ML348 was protective in non-diabetic unilateral ureteral obstruction and ischemia/reperfusion fibrosis models [73]. These findings identify the renal cell population, protein substrate and disease model as essential considerations for interpreting APT1 modulation, providing a mechanistic basis for evaluating cell- and substrate-selective approaches [17,73].

Drug studies vary in how directly they connect protection to CD36. Astragaloside IV reduced CD36, lipid accumulation, and NLRP3-associated inflammation in diabetic rats and lipid-stressed HK-2 cells, with CD36 overexpression weakening cellular protection [74]. Colquhounia root tablet experiments similarly used receptor overexpression to reverse selected apoptosis and autophagy-associated responses [32]. In TGF-β-exposed HK-2 cells, CD36 knockdown reduced profibrotic responses and limited further suppression by fisetin. CD36 overexpression increased those responses, but fisetin retained an effect; the animal model combined STZ-induced diabetes, LDL-receptor deficiency, and atherosclerosis [35]. These experiments provide functional evidence beyond a concurrent decrease in receptor expression, subject to the limitations of the models and intervention specificity summarized in Table 4.

Other studies focus on metabolic regulation or upstream signaling pathways. In a 2026 fibroblast growth factor 1 (FGF1) study, treatment lowered renal CD36, restored responses involving AMPK, PPARα, and carnitine palmitoyltransferase 1A (CPT1A), and improved respiration in high-glucose/palmitate-treated HK-2 cells. Pharmacological inhibition of

AMPK or FAO attenuated protection; direct CD36 knockdown or receptor rescue was not part of that test. Blood glucose and body weight also fell in the treated diabetic mice [75]. The pathway perturbations and respiration measurements support improved intracellular lipid handling as a component of the FGF1 response [75].

Table 4. Interpretation of intervention-associated CD36 changes.

Intervention Class	Representative Evidence	Supported Interpretation	Unresolved Questions
Genetic receptor perturbation	[6,29]	Functional contribution in the experimental animal or cell model	Local versus systemic effects, including lower glycemia; sustained efficacy and tolerability.
SSO pharmacology	[16,20,70,71]	Renal SSO-sensitive responses; nonrenal Lys164 binding and K164A functional tests; additional protein modification by SSO	Specificity in the renal assay; uptake versus metabolism; genetic confirmation.
Receptor antagonism in non-DKD CKD	[72]	The 5A apolipoprotein A-I mimetic peptide improved renal outcomes in wild-type mice without added benefit in *Cd36*-deficient mice.	Diabetic renal efficacy, cell specificity, and exclusive molecular targeting.
Upstream regulation or trafficking	[16,17,73]	*Dock5*/LXRα and APT1 manipulations affect receptor availability. APT1 increases CD36 ubiquitination in podocytes [17], but stabilizes β-catenin through Cys300 depalmitoylation in tubular cells [73].	CD36-specific mediation in vivo; cell and protein-substrate selectivity. Tubular *Apt1* deletion/ML348 protection was tested in non-diabetic UUO/IRI fibrosis [73], not in the podocyte DKD model.
Drug studies testing CD36 overexpression	[32,74]	Increased CD36 attenuated selected cellular drug effects	Whether CD36 is the only target and mediates benefit in vivo; autophagic flux where relevant.
Drug studies with additional CD36 perturbation	[35]	CD36 knockdown limited further suppression by fisetin; overexpression increased profibrotic responses, but fisetin retained an effect.	Validation in diabetic renal cells; distinction from systemic vascular effects.
Drug studies with associated expression change	[75–81]	CD36 changes during broader metabolic or antioxidant intervention; some studies test upstream pathway dependence	Whether the protective effect requires CD36.
Clinical measurements during treatment	[61]	Treatment-associated decreases in serum sCD36	Kidney origin, renal target engagement, causal mediation, and long-term prognostic value.

Table 4. *Cont.*

Intervention Class	Representative Evidence	Supported Interpretation	Unresolved Questions
Glucose-lowering drug experiments	[82–84]	CD36 responses in specified animal models, tissues, and analytes	Reproducible evidence of a renal CD36 effect; direct CD36 dependence cannot be inferred from drug-associated expression.

Across these categories, direct CD36 perturbation with functional readouts provides the most informative evidence of receptor dependence within each tested system. CD36 changes accompanying broader pharmacological treatment, and changes in circulating sCD36, remain indirect unless renal target engagement and receptor dependence are demonstrated. The cited human treatment evidence does not establish that clinical benefit is mediated by renal CD36, identifying a central translational gap. APT1, acyl-protein thioesterase 1; CD36, cluster of differentiation 36; CKD, chronic kidney disease; DKD, diabetic kidney disease; sCD36, soluble CD36; SSO, sulfo-N-succinimidyl oleate; UUO, unilateral ureteral obstruction; IRI, ischemia/reperfusion injury.

Studies of notoginsenoside R2 and PCSK9 inhibition tested the involvement of c-Src or AMPK and measured downstream changes in CD36 [76,77]. Studies of Qianshi mixture, isoquercitrin, and nanoemulsified garlic oil reported improvement alongside reductions in CD36-related measurements and broader metabolic changes [78–80]. An SS31 study in db/db mice and HK-2 cells exposed to high glucose reported improvements in markers of oxidative stress and renal injury together with lower CD36 expression [81]. These studies identify changes in CD36 during treatment. Restoring or suppressing CD36 during treatment would help determine whether those changes contribute to protection.

Antioxidant protection supports testing complementary interventions: mitoTEMPO attenuated CD36-enhanced NLRP3/IL-1β responses [29], while ferrostatin-1 protected a separate high-glucose/palmitate tubular model [18]. Whether either adds benefit to receptor modulation requires testing within the same system. Prioritization should consider receptor perturbation or reconstitution evidence, renal exposure, cell and substrate selectivity, and efficacy after injury is established (Table 4). Section 7.2 specifies the required causal comparisons.

6.3. Glucose-Lowering Drugs: Compartment and Model Dependence

Studies of sodium–glucose cotransporter 2 (SGLT2) inhibitors illustrate the importance of experimental context when interpreting CD36 responses. Empagliflozin reduced renal CD36 and lipid-related injury in high-fat-fed obese mice; pharmacological manipulation of PPARγ in palmitate-exposed HK-2 cells supported its role as an upstream regulator [82]. A dapagliflozin study in db/db mice combined renal RNA sequencing, network analysis, and protein measurements, identifying CD36 among treatment-responsive candidates. It reported lower renal CD36 in untreated diabetic mice and reversal toward control levels with treatment [83]. Neither study directly tested whether CD36 was required for the renal drug response and their divergent expression responses illustrate context-dependent patterns of CD36-associated treatment responses.

An experiment with exendin-4 showed increased CD36-related expression in brown adipose tissue while renal improvement persisted after removal of interscapular brown adipose tissue [84]. This adipose response and the serum sCD36 changes in Section 5.2 concern different analytes and compartments. Considered together, the adipose and circulating measurements illustrate the compartment-specific nature of CD36 responses to treatment.

6.4. Clinical Redox Interventions and Interpretation of Renal Outcomes

Clinical intervention in the NRF2 pathway illustrates why an improvement in an intermediate measure of kidney function does not necessarily translate into net clinical benefit. BEACON randomized 2185 patients with type 2 diabetes and stage 4 CKD to bardoxolone methyl or placebo and was stopped early. The primary composite of end-stage renal disease or cardiovascular death occurred in 69 patients in each group (hazard ratio 0.98; 95% confidence interval 0.70–1.37). Heart-failure hospitalization or death occurred in 96 versus 55 patients (hazard ratio 1.83; 95% confidence interval 1.32–2.55), despite an increase in estimated GFR with bardoxolone [28].

BEACON informs the choice of renal endpoints and safety assessments, although it does not test a CD36 mechanism. Development of CD36-directed treatments should likewise assess sustained renal outcomes and cardiovascular safety alongside target engagement in the kidney. The contrasting NRF2 models further support measuring metabolic and antioxidant effects concurrently.

7. Integrated Interpretation and Research Priorities

The conditional model in Figure 5 integrates receptor availability, ligand handling and signaling, intracellular lipid processing, and peroxide defense across the experimental systems discussed [16–18,29]. CD36-independent uptake and lipid accumulation without a full fibrotic phenotype delimit the conditions in which receptor modulation is expected to matter [5,23]. Under matched metabolic exposure, protection driven primarily by reduced substrate loading predicts that lower labeled-substrate entry will precede improvement in oxidant and injury measurements. Protection by a redox intervention despite unchanged substrate entry would show that injury can be reduced without lowering measured uptake. Concurrent assessment of ligand-triggered signaling would help distinguish uptake-related from signaling-associated effects. A factorial comparison of receptor modulation and antioxidant treatment in the same renal cell population could distinguish overlapping from additional protection. Together, these comparisons provide an experimental framework for distinguishing the roles of substrate entry, receptor signaling and redox protection in renal injury.

7.1. Cellular Localization and Disease Stage

The most consequential disagreement concerns the presence and activity of tubular CD36. Positive human staining and receptor-dependent cell experiments coexist with limited expression in some diabetic mouse models and absent proximal tubular staining in the KIM-1 study [19,22]. Whole-kidney *Cd36* mRNA was also reduced in a study of 32-week-old db/db mice, and the dapagliflozin report associated renal improvement with restoration of a reduced CD36 signal [83,85]. Interpreting these opposing results requires direct comparison of the models and measurements used.

A useful comparison would measure transcript abundance, total protein and membrane protein in the same identified cell populations, using validated antibodies and positive controls. Disease stage, epithelial differentiation, treatment and the proportions of epithelial and immune cells are candidate explanations for variation in bulk CD36 signals. Substrate presentation also matters: albumin-bound palmitate, unbound fatty acid preparations, oxidized lipoproteins and glycated proteins probe different receptor functions. Coordinated assessment of these variables would help relate tissue-level differences to CD36 localization and function in defined renal cell populations.

The contrasting uptake and storage findings in Figure 2 inform these comparisons, which would help identify where CD36 function reproducibly contributes to injury and which disease stages and cell populations are suitable for intervention.

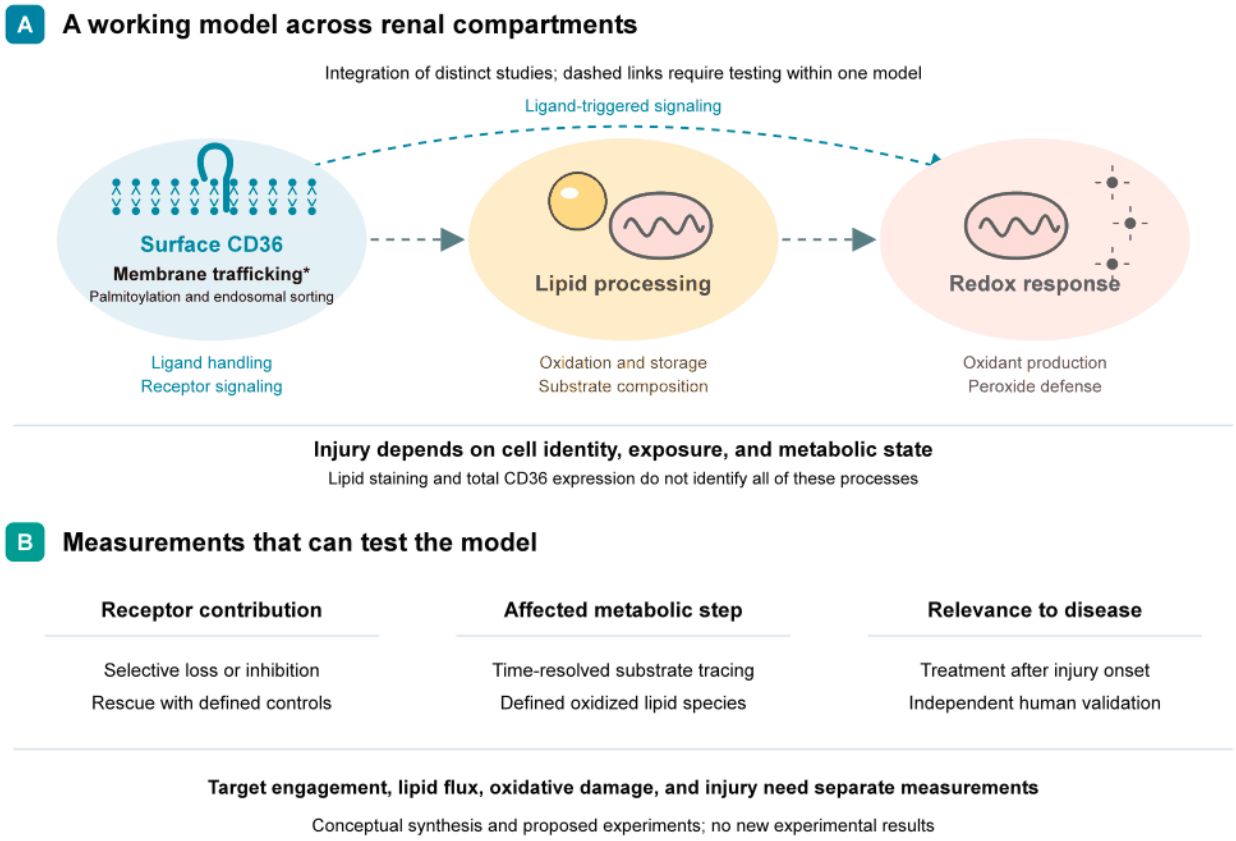


Figure 5. A conditional model of CD36-associated injury and experiments to test it. (**A**) Integration of receptor availability, lipid processing, and redox responses across distinct podocyte and tubular systems [16–18,29]. Dashed arrows mark connections requiring joint testing within one system. The curved arrow represents ligand-triggered signaling without requiring increased lipid storage as an intermediate [19,41]. Alternative uptake and the dissociation of storage from fibrosis constrain the model [5,23]. (**B**) Proposed measurements for establishing receptor dependence, identifying the affected metabolic step, and testing disease relevance. Rescue controls depend on the question: trafficking studies quantify surface abundance as an outcome while accounting for total protein; comparisons of membrane transport or signaling must account for surface abundance. Prospective validation in humans remains necessary. CD36, cluster of differentiation 36. The membrane-trafficking label summarizes palmitoylation- and compartment-localization evidence; direct trafficking rates were not measured.

7.2. Receptor Function and Causal Testing

Inducible *Cd36* deletion in tubular cells, podocytes, and renal myeloid populations would distinguish developmental or systemic effects from receptor function during established diabetes. Reconstitution with wild-type CD36 or variants affecting membrane localization could then test how receptor availability changes substrate handling, ligand signaling, and injury. This design would combine the cell specificity of the *Dock5* experiments with the receptor-variant approach used in the APT1 study within a single diabetic animal model [16,17]. Manipulation of CD36 in a defined renal compartment is feasible in other settings: inducible Pax8–rtTA-driven human CD36 expression aggravated folic-acid injury, although that non-DKD overexpression model differs from endogenous regulation in diabetes [86].

The expression controls should match the causal question. To test membrane trafficking, total receptor abundance should be controlled or its differences quantified, while surface abundance remains a mechanistic outcome; forcing equal surface abundance could conceal the trafficking effect. To compare transport or signaling at the membrane, surface

abundance should instead be matched or its contribution otherwise accounted for. Responsiveness to ligands and localization must be verified in either design. Restoration of uptake and injury supports receptor dependence but does not, by itself, distinguish transport from signaling. Concurrent substrate tracing and signaling measurements, supported by independently characterized functional variants, would help resolve this distinction. Glucose, fatty acid presentation, albumin binding, and osmotic controls should be matched across experimental groups.

A key experimental requirement is direct measurement of CD36 membrane-trafficking kinetics; immunofluorescence colocalization alone cannot establish flux between compartments. Time-resolved surface-label pulse–chase or biotinylation, antibody-feeding assays for internalization and recycling, or validated live-cell tracking should quantify internalization, recycling to the surface, surface residence, and lysosomal delivery, with total and cell-surface CD36 measured in parallel. Coupling these measurements to substrate tracing and redox-injury endpoints would establish which trafficking step changes and whether it precedes altered lipid flux or injury [17]. Endogenous Cys466 regulation and the effects of APT1 on other protein substrates should be assessed alongside these trafficking measurements.

Metabolic studies should combine isotope tracing and lipidomics with measurements of surface CD36, respiration, and injury. Glutathione, GPX4 abundance and catalytic activity, and defined lipid-peroxide species would help separate impaired peroxide removal from altered oxidant production. Protection by iron chelation, together with complementary genetic experiments, would strengthen the evidence for ferroptosis beyond that provided by a single inhibitor or marker. Mitochondrial oxidants, inflammasome activation, and ferroptotic death should remain distinct outcomes. A study of cisplatin-induced acute kidney injury linked CD36 to ubiquitination and degradation of ferroptosis suppressor protein 1 (FSP1); testing that route in DKD is a separate priority [87].

Temporally controlled renal *Nrf2* manipulation combined with *Cd36* deletion or expression-matched rescue could separate lipid-handling effects from antioxidant defense. Glycemia and blood pressure require concurrent measurement because both changed in the study using global *Nrf2* deletion in db/db mice; circulating lipids should also be monitored. Repeating the design across diabetic backgrounds would test whether the response depends on obesity or insulin deficiency [26,27].

The contributions of immune and endothelial cells require cell-specific investigation. Single-cell studies identify macrophage states for functional investigation [50,51], while mesangial cultures identify a candidate calcium-signaling response [42]. Spatial localization and cell-specific intervention could establish where these interactions occur. Replication should prespecify sex, diabetic background, and disease stage, with randomization and blinded outcome assessment, rather than relying on one exposure and one renal endpoint.

7.3. Clinical Validation and Intended Use

Clinical validation should start with a defined intended use. The existing studies address discrimination between disease categories, association with historical eGFR decline, or treatment-associated change [57,59,61,62]. These findings support different development paths; opposing serum associations further require assays and populations to be evaluated separately [60].

A prospective cohort study should prespecify the analyte and sample-handling procedures, measure CD36 before follow-up for the outcome begins, and assess whether it adds prognostic information beyond eGFR, UACR, glycemia, and treatment. Cellular measurements require assessment of sample composition; protein immunoassays require harmonized calibration and dilution procedures. External validation should use independent participants and evaluate calibration as well as discrimination. A proposed clinical

threshold should also show whether its use improves decisions beyond routine measures. For a treatment-response application, within-person variability, the molecular form detected, and the timing of change would need characterization before a fall in sCD36 could guide care.

Therapeutic studies should define the renal cell target, timing of intervention, background treatment and intended clinical outcome. Target engagement should be demonstrated with an assay suited to the intervention. For expression-based readouts, surface localization and functional measurements should accompany total CD36 abundance. These measurements can be assessed alongside circulating lipids, glycemia, blood pressure and immune function to characterize renal and systemic responses [2]. Demonstrating efficacy after injury is established, followed by independent human validation, would provide a staged route from renal target engagement to evaluation of sustained clinical benefit.

8. Conclusions

Experimental studies implicate CD36 in renal injury through functions that depend on cellular and metabolic context. Podocyte studies support regulated membrane availability as a determinant of lipid-associated injury, while tubular studies link receptor perturbation to oxidative metabolism, mitochondrial oxidant signaling, and cytokine-amplified lipid peroxidation. Interpreting these effects requires considering receptor function alongside the cell's capacity to metabolize incoming lipids and limit peroxide damage.

This synthesis favors testing selective receptor modulation in the affected renal compartment, with lipid flux and redox injury measured together. The responses of different protein substrates to trafficking regulators make cell and substrate selectivity a central consideration. Antioxidant rescue supports evaluating redox protection alongside receptor interventions, while human studies identify candidate CD36 measurements for evaluation in defined diagnostic, prognostic and treatment-response settings.

The immediate priority is to determine whether cell-specific CD36 manipulation and rescue produce sustained benefit after diabetic injury has developed. Establishing this link would strengthen the rationale for selecting CD36-directed and antioxidant interventions for subsequent clinical investigation.

Supplementary Materials: The following supporting information can be downloaded at: https://www.mdpi.com/article/10.3390/antiox15111479/s1, Supplementary Table S1: Relationship of the present synthesis to closely related re-views; Supplementary Table S2: Roles and renal compartments of recurring transcriptomic datasets.

Author Contributions: Writing—original draft, H.C.; Investigation, Writing—review and editing, C.H.; Supervision, T.L.; Funding acquisition, T.L. All authors have read and agreed to the published version of the manuscript.

Funding: This work was supported by the Ningxia Natural Science Foundation (Outstanding Young Scholars Project), Department of Science and Technology of Ningxia Hui Autonomous Region (grant No. 2023AAC05032); the Special Talent Start-up Project of Ningxia Medical University (grant No. XT2022027); the Open Project of the Key Laboratory of Dryness Syndrome in Chinese Medicine, Ministry of Education, Ningxia Medical University; and the National Natural Science Foundation of China (grant No. 82661062); 2026 College Student Innovation and Entrepreneurship Training Program (Provincial Level) (S202610752066).

Institutional Review Board Statement: Not applicable.

Informed Consent Statement: Not applicable.

Data Availability Statement: No new datasets were generated. The sources considered in this review are identified in the reference list and Supplementary Materials.

Acknowledgments: OpenAI Codex (GPT-6) assisted with literature organization and language translation. The author team first classified and thematically grouped the bibliographic records retrieved through database searches and selected for inclusion. The authors manually checked every cited reference against its original publication, verifying author names, article titles, journal names, publication years, volume and issue, page ranges, and DOIs. Two authors independently reviewed the content after AI-assisted literature organization and language editing. They checked the accuracy of the literature classification, whether language editing preserved the original meaning, and the completeness of the reference information.

Conflicts of Interest: The authors declare no conflicts of interest. The funding bodies provided financial support only and had no role in the design of this review; the collection, analysis, or interpretation of the literature; the writing of the manuscript; or the decision to submit it for publication.

Abbreviations

AAV, adeno-associated virus; ACSL4, acyl-CoA synthetase long-chain family member 4; AMPK, AMP-activated protein kinase; AOPPs, advanced oxidation protein products; APT1, acyl-protein thioesterase 1; CD36, cluster of differentiation 36; CKD, chronic kidney disease; CMV, cytomegalovirus; CPT1A, carnitine palmitoyltransferase 1A; CXCL16, C-X-C motif chemokine ligand 16; DHE, dihydroethidium; DKD, diabetic kidney disease; DN, diabetic nephropathy; ECAR, extracellular acidification rate; eGFR, estimated glomerular filtration rate; ELISA, enzyme-linked immunosorbent assay; ER, endoplasmic reticulum; ERK, extracellular signal-regulated kinase; FAO, fatty acid oxidation; FGF1, fibroblast growth factor 1; FSP1, ferroptosis suppressor protein 1; GLP-1, glucagon-like peptide-1; GPX4, glutathione peroxidase 4; GSH, glutathione; HFD, high-fat diet; HODE, hydroxyoctadecadienoic acid; IL-1β, interleukin-1β; IL-6, interleukin-6; IRI, ischemia/reperfusion injury; JAK, Janus kinase; KIM-1, kidney injury molecule-1; LAMP1, lysosome-associated membrane protein 1; LC3, microtubule-associated protein 1 light chain 3; LDL, low-density lipoprotein; LXRα, liver X receptor α; m^6A, N^6-methyladenosine; MDA, malondialdehyde; mtROS, mitochondrial reactive oxygen species; NF-κB, nuclear factor κB; NFAT2, nuclear factor of activated T cells 2; NLRP3, NLR family pyrin domain-containing 3; NRF2, nuclear factor erythroid 2-related factor 2; PCSK9, proprotein convertase subtilisin/kexin type 9; PPAR, peroxisome proliferator-activated receptor; ROS, reactive oxygen species; sCD36, soluble CD36; SGLT2, sodium–glucose cotransporter 2; shRNA, short hairpin RNA; siRNA, small interfering RNA; SSO, sulfo-N-succinimidyl oleate; STAT3, signal transducer and activator of transcription 3; STZ, streptozotocin; T1D/T2D, type 1/type 2 diabetes; TGF-β, transforming growth factor-β; TREM2, triggering receptor expressed on myeloid cells 2; TRPC6, transient receptor potential canonical channel 6; TSP1, thrombospondin-1; UACR, urine albumin-to-creatinine ratio; UUO, unilateral ureteral obstruction; WGCNA, weighted gene coexpression network analysis; YTHDF2, YTH domain family protein 2; ZEB1, zinc finger E-box-binding homeobox 1.

References

1. Mitrofanova, A.; Burke, G.; Merscher, S.; Fornoni, A. New insights into renal lipid dysmetabolism in diabetic kidney disease. *World J. Diabetes* **2021**, *12*, 524–540. [CrossRef] [PubMed]
2. Puchałowicz, K.; Rać, M.E. The Multifunctionality of CD36 in Diabetes Mellitus and Its Complications-Update in Pathogenesis, Treatment and Monitoring. *Cells* **2020**, *9*, 1877. [CrossRef] [PubMed]
3. Gai, Z.; Wang, T.; Visentin, M.; Kullak-Ublick, G.A.; Fu, X.; Wang, Z. Lipid Accumulation and Chronic Kidney Disease. *Nutrients* **2019**, *11*, 722. [CrossRef] [PubMed]
4. Lin, P.H.; Duann, P. Dyslipidemia in Kidney Disorders: Perspectives on Mitochondria Homeostasis and Therapeutic Opportunities. *Front. Physiol.* **2020**, *11*, 1050. [CrossRef] [PubMed]
5. Scerbo, D.; Son, N.H.; Sirwi, A.; Zeng, L.; Sas, K.M.; Cifarelli, V.; Schoiswohl, G.; Huggins, L.A.; Gumaste, N.; Hu, Y.; et al. Kidney triglyceride accumulation in the fasted mouse is dependent upon serum free fatty acids. *J. Lipid Res.* **2017**, *58*, 1132–1142. [CrossRef] [PubMed]
6. Niu, H.; Ren, X.; Tan, E.; Wan, X.; Wang, Y.; Shi, H.; Hou, Y.; Wang, L. CD36 deletion ameliorates diabetic kidney disease by restoring fatty acid oxidation and improving mitochondrial function. *Ren. Fail* **2023**, *45*, 2292753. [CrossRef] [PubMed]
7. Yang, X.; Okamura, D.M.; Lu, X.; Chen, Y.; Moorhead, J.; Varghese, Z.; Ruan, X.Z. CD36 in chronic kidney disease: Novel insights and therapeutic opportunities. *Nat. Rev. Nephrol.* **2017**, *13*, 769–781. [CrossRef] [PubMed]

8. Chae, S.Y.; Kim, Y.; Park, C.W. Oxidative Stress Induced by Lipotoxicity and Renal Hypoxia in Diabetic Kidney Disease and Possible Therapeutic Interventions: Targeting the Lipid Metabolism and Hypoxia. *Antioxidants* **2023**, *12*, 2083. [CrossRef] [PubMed]
9. Wang, N.; Zhang, C. Oxidative Stress: A Culprit in the Progression of Diabetic Kidney Disease. *Antioxidants* **2024**, *13*, 455. [CrossRef] [PubMed]
10. Dong, Y.; Tong, Y. Lipid Peroxidation in Diabetic Kidney Disease: Mechanism and Natural Solution. *Int. J. Mol. Sci.* **2025**, *26*, 9764. [CrossRef] [PubMed]
11. Zou, Z.; Gao, P.; Yuan, Q.; Wang, Z.; Luo, P.; Zhang, C. Fatty Kidney: The Interplay of Lipids and Diabetic Kidney Disease. *Biomedicines* **2026**, *14*, 944. [CrossRef] [PubMed]
12. Zaitoon, H.; Feigin, E.; Abdul-Ghani, M.; Clarke, G.D.; Tuttle, K.R.; DeFronzo, R.A. Renal Lipotoxicity: Mechanisms and Therapeutic Perspectives. *Diabetes Care* **2026**. [CrossRef] [PubMed]
13. Pi, Y.; Wen, L.; Cheng, X.; Tang, X. Rewiring lipid metabolism in diabetic kidney disease: Pathogenic networks and the therapeutic convergence of natural products. *Pathol. Res. Pract.* **2026**, *286*, 156604. [CrossRef] [PubMed]
14. Zhou, L.; Shen, X.L.; Zhu, Q.R.; Yu, W.K.; Li, H.C.; Cao, G.; Bao, Y.N. Targeting posttranslational modifications of oxidative stress pathways for the treatment of diabetic nephropathy. *J. Pharm. Anal.* **2026**, *16*, 101558. [CrossRef] [PubMed]
15. Li, M.; Zhu, H.; Zhao, H.; Liu, C.; Wang, Y.; Zuo, L. Post-translational protein S-palmitoylation in renal tubular injury: Mechanisms and therapeutic implications. *Front. Cell Dev. Biol.* **2026**, *14*, 1960988. [CrossRef] [PubMed]
16. Qu, H.; Liu, X.; Zhu, J.; Xiong, X.; Li, L.; He, Q.; Wang, Y.; Yang, G.; Zhang, L.; Yang, Q.; et al. Dock5 Deficiency Promotes Proteinuric Kidney Diseases via Modulating Podocyte Lipid Metabolism. *Adv. Sci.* **2024**, *11*, e2306365. [CrossRef] [PubMed]
17. Wang, J.; Hu, J.; Hu, H.; Guan, Q.; Zhu, Z.; Yang, Q.; Ding, G. APT1-derived depalmitoylation of CD36 alleviates diabetes-induced lipotoxicity in podocytes. *Int. J. Biol. Sci.* **2025**, *21*, 3852–3866. [CrossRef] [PubMed]
18. Wang, X.; Wan, J.; Wang, C.; Tong, Y.; Chen, Y.; Wang, X.; Liu, J.; Li, Q.; Dong, Z.; Hong, Q.; et al. Trem2+ Macrophages Alleviate Renal Tubule Lipid Accumulation and Ferroptosis in Diabetic Nephropathy by Repressing IL-1β-Mediated CD36 Expression. *Diabetes* **2025**, *74*, 2231–2248. [CrossRef] [PubMed]
19. Susztak, K.; Ciccone, E.; McCue, P.; Sharma, K.; Böttinger, E.P. Multiple metabolic hits converge on CD36 as novel mediator of tubular epithelial apoptosis in diabetic nephropathy. *PLoS Med.* **2005**, *2*, e45. [CrossRef] [PubMed]
20. Hua, W.; Huang, H.Z.; Tan, L.T.; Wan, J.M.; Gui, H.B.; Zhao, L.; Ruan, X.Z.; Chen, X.M.; Du, X.G. CD36 Mediated Fatty Acid-Induced Podocyte Apoptosis via Oxidative Stress. *PLoS ONE* **2015**, *10*, e0127507. [CrossRef] [PubMed]
21. Gutwein, P.; Abdel-Bakky, M.S.; Doberstein, K.; Schramme, A.; Beckmann, J.; Schaefer, L.; Amann, K.; Doller, A.; Kämpfer-Kolb, N.; Abdel-Aziz, A.H.; et al. CXCL16 and oxLDL are induced in the onset of diabetic nephropathy. *J. Cell Mol. Med.* **2009**, *13*, 3809–3825. [CrossRef] [PubMed]
22. Mori, Y.; Ajay, A.K.; Chang, J.H.; Mou, S.; Zhao, H.; Kishi, S.; Li, J.; Brooks, C.R.; Xiao, S.; Woo, H.M.; et al. KIM-1 mediates fatty acid uptake by renal tubular cells to promote progressive diabetic kidney disease. *Cell Metab.* **2021**, *33*, 1042–1061.e7. [CrossRef] [PubMed]
23. Kang, H.M.; Ahn, S.H.; Choi, P.; Ko, Y.A.; Han, S.H.; Chinga, F.; Park, A.S.; Tao, J.; Sharma, K.; Pullman, J.; et al. Defective fatty acid oxidation in renal tubular epithelial cells has a key role in kidney fibrosis development. *Nat. Med.* **2015**, *21*, 37–46. [CrossRef] [PubMed]
24. Feng, L.; Gu, C.; Li, Y.; Huang, J. High Glucose Promotes CD36 Expression by Upregulating Peroxisome Proliferator-Activated Receptor γ Levels to Exacerbate Lipid Deposition in Renal Tubular Cells. *BioMed Res. Int.* **2017**, *2017*, 1414070. [CrossRef] [PubMed]
25. Byun, J.H.; Lebeau, P.F.; Platko, K.; Carlisle, R.E.; Faiyaz, M.; Chen, J.; MacDonald, M.E.; Makda, Y.; Yousof, T.; Lynn, E.G.; et al. Inhibitory Antibodies against PCSK9 Reduce Surface CD36 and Mitigate Diet-Induced Renal Lipotoxicity. *Kidney360* **2022**, *3*, 1394–1410. [CrossRef] [PubMed]
26. Su, K.; Zhao, S.L.; Yang, W.X.; Lo, C.S.; Chenier, I.; Liao, M.C.; Pang, Y.C.; Peng, J.Z.; Miyata, K.N.; Cailhier, J.F.; et al. NRF2 Deficiency Attenuates Diabetic Kidney Disease in Db/Db Mice via Down-Regulation of Angiotensinogen, SGLT2, CD36, and FABP4 Expression and Lipid Accumulation in Renal Proximal Tubular Cells. *Antioxidants* **2023**, *12*, 1715. [CrossRef] [PubMed]
27. Liu, Y.; Uruno, A.; Saito, R.; Matsukawa, N.; Hishinuma, E.; Saigusa, D.; Liu, H.; Yamamoto, M. Nrf2 deficiency deteriorates diabetic kidney disease in Akita model mice. *Redox Biol.* **2022**, *58*, 102525. [CrossRef] [PubMed]
28. de Zeeuw, D.; Akizawa, T.; Audhya, P.; Bakris, G.L.; Chin, M.; Christ-Schmidt, H.; Goldsberry, A.; Houser, M.; Krauth, M.; Lambers Heerspink, H.J.; et al. Bardoxolone methyl in type 2 diabetes and stage 4 chronic kidney disease. *N. Engl. J. Med.* **2013**, *369*, 2492–2503. [CrossRef] [PubMed]
29. Hou, Y.; Wang, Q.; Han, B.; Chen, Y.; Qiao, X.; Wang, L. CD36 promotes NLRP3 inflammasome activation via the mtROS pathway in renal tubular epithelial cells of diabetic kidneys. *Cell Death Dis.* **2021**, *12*, 523. [CrossRef] [PubMed]
30. Cao, W.; Xu, J.; Zhou, Z.M.; Wang, G.B.; Hou, F.F.; Nie, J. Advanced oxidation protein products activate intrarenal renin-angiotensin system via a CD36-mediated, redox-dependent pathway. *Antioxid. Redox Signal* **2013**, *18*, 19–35. [CrossRef] [PubMed]

31. Li, X.; Zhang, T.; Geng, J.; Wu, Z.; Xu, L.; Liu, J.; Tian, J.; Zhou, Z.; Nie, J.; Bai, X. Advanced Oxidation Protein Products Promote Lipotoxicity and Tubulointerstitial Fibrosis via CD36/β-Catenin Pathway in Diabetic Nephropathy. *Antioxid. Redox Signal* **2019**, *31*, 521–538. [CrossRef] [PubMed]
32. Li, H.; Wang, B.; Wu, C.; Xie, D.; Li, J.; Wang, N.; Chen, H.; Liu, L. Colquhounia Root Tablet Promotes Autophagy and Inhibits Apoptosis in Diabetic Nephropathy by Suppressing CD36 Expression In Vivo and In Vitro. *J. Diabetes Res.* **2023**, *2023*, 4617653. [CrossRef] [PubMed]
33. Okamura, D.M.; Pennathur, S.; Pasichnyk, K.; López-Guisa, J.M.; Collins, S.; Febbraio, M.; Heinecke, J.; Eddy, A.A. CD36 regulates oxidative stress and inflammation in hypercholesterolemic CKD. *J. Am. Soc. Nephrol.* **2009**, *20*, 495–505. [CrossRef] [PubMed]
34. Ruan, Y.; Yuan, P.P.; Wei, Y.X.; Zhang, Q.; Gao, L.Y.; Li, P.Y.; Chen, Y.; Fu, Y.; Cao, Y.G.; Zheng, X.K.; et al. Phenolic Compounds from Mori Cortex Ameliorate Sodium Oleate-Induced Epithelial-Mesenchymal Transition and Fibrosis in NRK-52e Cells through CD36. *Molecules* **2021**, *26*, 6133. [CrossRef] [PubMed]
35. Zou, T.F.; Liu, Z.G.; Cao, P.C.; Zheng, S.H.; Guo, W.T.; Wang, T.X.; Chen, Y.L.; Duan, Y.J.; Li, Q.S.; Liao, C.Z.; et al. Fisetin treatment alleviates kidney injury in mice with diabetes-exacerbated atherosclerosis through inhibiting CD36/fibrosis pathway. *Acta Pharmacol. Sin.* **2023**, *44*, 2065–2074. [CrossRef] [PubMed]
36. Xu, S.; Nam, S.M.; Kim, J.H.; Das, R.; Choi, S.K.; Nguyen, T.T.; Quan, X.; Choi, S.J.; Chung, C.H.; Lee, E.Y.; et al. Palmitate induces ER calcium depletion and apoptosis in mouse podocytes subsequent to mitochondrial oxidative stress. *Cell Death Dis.* **2015**, *6*, e1976. [CrossRef] [PubMed]
37. Hua, W.; Peng, L.; Chen, X.M.; Jiang, X.; Hu, J.; Jiang, X.H.; Xiang, X.; Wan, J.; Long, Y.; Xiong, J.; et al. CD36-mediated podocyte lipotoxicity promotes foot process effacement. *Open Med.* **2024**, *19*, 20240918. [CrossRef] [PubMed]
38. Zhao, J.; Rui, H.L.; Yang, M.; Sun, L.J.; Dong, H.R.; Cheng, H. CD36-Mediated Lipid Accumulation and Activation of NLRP3 Inflammasome Lead to Podocyte Injury in Obesity-Related Glomerulopathy. *Mediat. Inflamm.* **2019**, *2019*, 3172647. [CrossRef] [PubMed]
39. Yang, X.; Wu, Y.; Li, Q.; Zhang, G.; Wang, M.; Yang, H.; Li, Q. CD36 Promotes Podocyte Apoptosis by Activating the Pyrin Domain-Containing-3 (NLRP3) Inflammasome in Primary Nephrotic Syndrome. *Med. Sci. Monit.* **2018**, *24*, 6832–6839. [CrossRef] [PubMed]
40. Maimaitiyiming, H.; Zhou, Q.; Wang, S. Thrombospondin 1 Deficiency Ameliorates the Development of Adriamycin-Induced Proteinuric Kidney Disease. *PLoS ONE* **2016**, *11*, e0156144. [CrossRef] [PubMed]
41. Cui, W.; Maimaitiyiming, H.; Zhou, Q.; Norman, H.; Zhou, C.; Wang, S. Interaction of thrombospondin1 and CD36 contributes to obesity-associated podocytopathy. *Biochim. Biophys. Acta* **2015**, *1852*, 1323–1333. [CrossRef] [PubMed]
42. Su, Y.; Chen, Q.; Ju, Y.; Li, W.; Li, W. Palmitate induces human glomerular mesangial cells fibrosis through CD36-mediated transient receptor potential canonical channel 6/nuclear factor of activated T cell 2 activation. *Biochim. Biophys. Acta Mol. Cell Biol. Lipids* **2020**, *1865*, 158793. [CrossRef] [PubMed]
43. Su, Y.; Chen, Q.; Ma, K.; Ju, Y.; Ji, T.; Wang, Z.; Li, W.; Li, W. Astragaloside IV inhibits palmitate-mediated oxidative stress and fibrosis in human glomerular mesangial cells via downregulation of CD36 expression. *Pharmacol. Rep.* **2019**, *71*, 319–329. [CrossRef] [PubMed]
44. Lee, E.; Choi, J.; Lee, H.S. Palmitate induces mitochondrial superoxide generation and activates AMPK in podocytes. *J. Cell Physiol.* **2017**, *232*, 3209–3217. [CrossRef] [PubMed]
45. Doll, S.; Proneth, B.; Tyurina, Y.Y.; Panzilius, E.; Kobayashi, S.; Ingold, I.; Irmler, M.; Beckers, J.; Aichler, M.; Walch, A.; et al. ACSL4 dictates ferroptosis sensitivity by shaping cellular lipid composition. *Nat. Chem. Biol.* **2017**, *13*, 91–98. [CrossRef] [PubMed]
46. Kagan, V.E.; Mao, G.; Qu, F.; Angeli, J.P.; Doll, S.; Croix, C.S.; Dar, H.H.; Liu, B.; Tyurin, V.A.; Ritov, V.B.; et al. Oxidized arachidonic and adrenic PEs navigate cells to ferroptosis. *Nat. Chem. Biol.* **2017**, *13*, 81–90. [CrossRef] [PubMed]
47. Murphy, M.P.; Bayir, H.; Belousov, V.; Chang, C.J.; Davies, K.J.A.; Davies, M.J.; Dick, T.P.; Finkel, T.; Forman, H.J.; Janssen-Heininger, Y.; et al. Guidelines for measuring reactive oxygen species and oxidative damage in cells and in vivo. *Nat. Metab.* **2022**, *4*, 651–662. [CrossRef] [PubMed]
48. Stewart, C.R.; Stuart, L.M.; Wilkinson, K.; van Gils, J.M.; Deng, J.; Halle, A.; Rayner, K.J.; Boyer, L.; Zhong, R.; Frazier, W.A.; et al. CD36 ligands promote sterile inflammation through assembly of a Toll-like receptor 4 and 6 heterodimer. *Nat. Immunol.* **2010**, *11*, 155–161. [CrossRef] [PubMed]
49. Sheedy, F.J.; Grebe, A.; Rayner, K.J.; Kalantari, P.; Ramkhelawon, B.; Carpenter, S.B.; Becker, C.E.; Ediriweera, H.N.; Mullick, A.E.; Golenbock, D.T.; et al. CD36 coordinates NLRP3 inflammasome activation by facilitating intracellular nucleation of soluble ligands into particulate ligands in sterile inflammation. *Nat. Immunol.* **2013**, *14*, 812–820. [CrossRef] [PubMed]
50. Zhang, B.; Wu, Y.; Wang, Z.; Gao, S.; Liu, H.; Lin, Y.; Yu, P. Unveiling macrophage dynamics and efferocytosis-related targets in diabetic kidney disease: Insights from single-cell and bulk RNA-sequencing. *Front. Immunol.* **2025**, *16*, 1521554. [CrossRef] [PubMed]
51. Yang, X.; Li, J.; Zeng, Y.; Wang, G.; Zeng, J.; Liu, D. Integrated single-cell transcriptomic and machine-learning analyses identify a CD36-associated macrophage state in diabetic nephropathy. *Front. Immunol.* **2026**, *17*, 1868468. [CrossRef] [PubMed]

52. Yang, P.; Xiao, Y.; Luo, X.; Zhao, Y.; Zhao, L.; Wang, Y.; Wu, T.; Wei, L.; Chen, Y. Inflammatory stress promotes the development of obesity-related chronic kidney disease via CD36 in mice. *J. Lipid Res.* **2017**, *58*, 1417–1427. [CrossRef] [PubMed]
53. Munkonda, M.N.; Akbari, S.; Landry, C.; Sun, S.; Xiao, F.; Turner, M.; Holterman, C.E.; Nasrallah, R.; Hébert, R.L.; Kennedy, C.R.J.; et al. Podocyte-derived microparticles promote proximal tubule fibrotic signaling via p38 MAPK and CD36. *J. Extracell. Vesicles* **2018**, *7*, 1432206. [CrossRef] [PubMed]
54. Ghanem, S.K.; Abdelsalam, S.S.; Bader, L.; Agouni, A. Large extracellular vesicles (microvesicles) in diabetic nephropathy: A systematic review of preclinical studies. *Front. Pharmacol.* **2025**, *16*, 1622280. [CrossRef] [PubMed]
55. Herman-Edelstein, M.; Scherzer, P.; Tobar, A.; Levi, M.; Gafter, U. Altered renal lipid metabolism and renal lipid accumulation in human diabetic nephropathy. *J. Lipid Res.* **2014**, *55*, 561–572. [CrossRef] [PubMed]
56. Jiang, H.; Geng, M.H.; Zhan, Y.M.; Shen, J.F.; Wang, F.Z.; Lin, S.Q.; Hong, Z.; Guo, C.H.; Deng, J.X.; Wu, S.C. Identification and validation of energy metabolism-related genes in diabetic kidney disease through integrated bioinformatics and in vivo analysis. *Hereditas* **2026**, *163*, 33. [CrossRef] [PubMed]
57. Zocchio, T.T.; Santos, A.S.; Cavaleiro, A.M.; Matheus, L.H.G.; de Fátima Mello Santana, M.; Palanca, E.; Rodrigues, A.T.; Vancini, M.G.; Nery, M.; Passarelli, M.; et al. Gene Expression in Urinary Sediment Cells as an Indicator of the Contribution of Plasma Lipids to Diabetic Kidney Disease. *J. Diabetes Res.* **2025**, *2025*, 2349928. [CrossRef] [PubMed]
58. Shiju, T.M.; Mohan, V.; Balasubramanyam, M.; Viswanathan, P. Soluble CD36 in plasma and urine: A plausible prognostic marker for diabetic nephropathy. *J. Diabetes Complicat.* **2015**, *29*, 400–406. [CrossRef] [PubMed]
59. Moovendhan, I.G.; Roopa, A.K.; Karthick, E.; Ganesh, M.; Sowmya, K. Evaluation of Serum Soluble CD36 Levels in the Clinical Progression of Diabetic Nephropathy. *EJIFCC* **2025**, *36*, 475–483. [PubMed]
60. Wang, Y.T.; Guo, R.K.; Li, Z.C.; Zhang, R.; Li, L.; Li, H.Y.; Zhang, J.L.; Han, Q.Q.; Liu, F. Association of Serum Soluble CD36 with Clinical Variables in Diabetic Patients with Chronic Kidney Disease. *Sichuan DA Xue Xue Bao YI Xue Ban* **2018**, *49*, 414–419. [PubMed]
61. Li, W.; Wang, Y. The potential biomarker value of soluble CD36 in the treatment of diabetic kidney disease: Evidence from GLP-1 and insulin interventions. *Front. Endocrinol.* **2025**, *16*, 1605631. [CrossRef] [PubMed]
62. González-Luis, A.; Siverio-Morales, O.; Hernández-Carballo, C.; Mora-Fernández, C.; Martín-Núñez, E.; Reyes-Carrión, A.; Carlos-Monzón, J.D.; Navarro-González, J.F.; Donate-Correa, J. Inflammatory markers associated with albuminuria and early atherosclerosis in type 2 diabetic kidney disease: A cross-sectional study. *Front. Endocrinol.* **2026**, *17*, 1732900. [CrossRef] [PubMed]
63. Li, Y.; Chen, Y.; Ruan, X.Z. The association of soluble cluster of differentiation 36 with metabolic diseases: A potential biomarker and therapeutic target. *Pediatr. Discov.* **2023**, *1*, e9. [CrossRef] [PubMed]
64. Alkhatatbeh, M.J.; Enjeti, A.K.; Acharya, S.; Thorne, R.F.; Lincz, L.F. The origin of circulating CD36 in type 2 diabetes. *Nutr. Diabetes* **2013**, *3*, e59. [CrossRef] [PubMed]
65. Yan, Q.; Du, Y.; Huang, F.; Zhan, M.; Zheng, Q.; Zhang, Q.; Zhang, P.; Yan, J.; Wu, X.; Lin, H.; et al. Copper metabolism-related biomarkers and therapeutic targets for diabetic nephropathy. *PeerJ* **2025**, *13*, e20468. [CrossRef] [PubMed]
66. Zhang, L.; Sun, Z.; Yuan, Y.; Sheng, J. Integrating bioinformatics and machine learning to identify glomerular injury genes and predict drug targets in diabetic nephropathy. *Sci. Rep.* **2025**, *15*, 16868. [CrossRef] [PubMed]
67. Xu, M.; Zhou, H.; Hu, P.; Pan, Y.; Wang, S.; Liu, L.; Liu, X. Identification and validation of immune and oxidative stress-related diagnostic markers for diabetic nephropathy by WGCNA and machine learning. *Front. Immunol.* **2023**, *14*, 1084531. [CrossRef] [PubMed]
68. Yan, Q.; Zhao, Z.; Liu, D.; Li, J.; Pan, S.; Duan, J.; Dong, J.; Liu, Z. Integrated analysis of potential gene crosstalk between non-alcoholic fatty liver disease and diabetic nephropathy. *Front. Endocrinol.* **2022**, *13*, 1032814. [CrossRef] [PubMed]
69. Liu, Y.; Huang, Y.; Su, Y.; Wang, L.; Lv, S.; Fu, Y.; Liu, Y.; Chang, B.; Ding, Y. Identification of key biomarkers for ferroptosis in diabetic kidney disease using machine learning and WGCNA. *Mol. Cell Endocrinol.* **2026**, *621*, 112877. [CrossRef] [PubMed]
70. Kuda, O.; Pietka, T.A.; Demianova, Z.; Kudova, E.; Cvacka, J.; Kopecky, J.; Abumrad, N.A. Sulfo-N-succinimidyl oleate (SSO) inhibits fatty acid uptake and signaling for intracellular calcium via binding CD36 lysine 164: SSO also inhibits oxidized low density lipoprotein uptake by macrophages. *J. Biol. Chem.* **2013**, *288*, 15547–15555. [CrossRef] [PubMed]
71. Jay, A.G.; Simard, J.R.; Huang, N.; Hamilton, J.A. SSO and other putative inhibitors of FA transport across membranes by CD36 disrupt intracellular metabolism, but do not affect FA translocation. *J. Lipid Res.* **2020**, *61*, 790–807. [CrossRef] [PubMed]
72. Souza, A.C.; Bocharov, A.V.; Baranova, I.N.; Vishnyakova, T.G.; Huang, Y.G.; Wilkins, K.J.; Hu, X.; Street, J.M.; Alvarez-Prats, A.; Mullick, A.E.; et al. Antagonism of scavenger receptor CD36 by 5A peptide prevents chronic kidney disease progression in mice independent of blood pressure regulation. *Kidney Int.* **2016**, *89*, 809–822. [CrossRef] [PubMed]
73. Gu, M.; Jiang, H.; Tan, M.; Yu, L.; Xu, N.; Li, Y.; Wu, H.; Hou, Q.; Dai, C. Palmitoyltransferase DHHC9 and acyl protein thioesterase APT1 modulate renal fibrosis through regulating β-catenin palmitoylation. *Nat. Commun.* **2023**, *14*, 6682. [CrossRef] [PubMed]

74. Li, X.; Dong, X.; Zhang, L.; Zhang, S.; Huang, W.; Wang, C.; Huo, Z.; Li, X.; Zhang, X.; Jia, X.; et al. Astragaloside IV attenuates renal tubule injury in DKD rats via suppression of CD36-mediated NLRP3 inflammasome activation. *Front. Pharmacol.* **2024**, *15*, 1285797. [CrossRef] [PubMed]
75. Li, Y.J.; Ge, H.Y.; Zhang, G.G.; Chen, H.Y.; Xi, Y.J.; Wang, K.; Huang, Y.L.; Zhang, C.; Fan, X.; Yan, X.Q. Fibroblast growth factor 1 alleviates diabetic nephropathy by reducing renal lipid accumulation in diabetic kidney. *World J. Diabetes* **2026**, *17*, 112475. [CrossRef] [PubMed]
76. Guo, X.; Yang, L.; An, X.; Hu, M.; Shen, Y.; Wang, N.; Xu, Y.; Gui, D. Protective effects of Notoginsenoside R2 on reducing lipid accumulation and mitochondrial dysfunction in diabetic nephropathy through regulation of c-Src. *Chin. Med.* **2025**, *20*, 10. [CrossRef] [PubMed]
77. Yang, K.J.; Lee, S.; Kim, S.; Youn, S.; Park, H.; Hwang, Y.; Han, S.; Chang, Y.K.; Park, C.W.; Hong, Y.A. PCSK9 Inhibition Attenuates Renal Oxidative Stress and Lipotoxicity in Diabetic Kidney Disease in Association with AMPK Activation. *Antioxidants* **2026**, *15*, 1182. [CrossRef] [PubMed]
78. Liu, J.; Liu, B.; Fan, E.; Zhang, H.; Yin, Z.; Lv, S.; Wen, W.; Min, F.; Zhang, Z.; Cui, H. Qianshi Mixture Treats Diabetic Nephropathy by Regulating Lipid Metabolism Reprogramming and Inhibiting Oxidative Stress Damage. *J. Cell Mol. Med.* **2025**, *29*, e70628. [CrossRef] [PubMed]
79. Wu, Q.; Tao, Y.; Sun, C.; Li, Y.; Liu, T.; Liu, B.; Li, W.; Gao, K.; Zhou, Y. Isoquercitrin Improves Renal Tubular Epithelial Cell Mitochondrial Dysfunction by Regulating Extracellular Signal-Regulated Kinase/Reactive Oxygen Species Signaling and Connexin 43 Expression in Diabetic Kidney Disease. *Phytother Res.* **2026**, *40*, 4988–5004. [CrossRef] [PubMed]
80. Yuvashree, M.; Ganesh, R.N.; Viswanathan, P. Potential application of nanoemulsified garlic oil blend in mitigating the progression of type 2 diabetes-mediated nephropathy in Wistar rats. *3 Biotech* **2020**, *10*, 272. [CrossRef] [PubMed]
81. Hou, Y.; Shi, Y.; Han, B.; Liu, X.; Qiao, X.; Qi, Y.; Wang, L. The antioxidant peptide SS31 prevents oxidative stress, downregulates CD36 and improves renal function in diabetic nephropathy. *Nephrol. Dial. Transpl.* **2018**, *33*, 1908–1918. [CrossRef] [PubMed]
82. Huang, C.C.; Chou, C.A.; Chen, W.Y.; Yang, J.L.; Lee, W.C.; Chen, J.B.; Lee, C.T.; Li, L.C. Empagliflozin Ameliorates Free Fatty Acid Induced-Lipotoxicity in Renal Proximal Tubular Cells via the PPARγ/CD36 Pathway in Obese Mice. *Int. J. Mol. Sci.* **2021**, *22*, 12408. [CrossRef] [PubMed]
83. Bai, Z.; Xie, T.; Liu, T.; Chen, Z.; Yu, L.; Zhang, C.; Luo, J.; Chen, L.; Zhao, X.; Xiao, Y. An integrated RNA sequencing and network pharmacology approach reveals the molecular mechanism of dapagliflozin in the treatment of diabetic nephropathy. *Front. Endocrinol.* **2022**, *13*, 967822. [CrossRef] [PubMed]
84. Fang, S.; Cai, Y.; Lyu, F.; Zhang, H.; Wu, C.; Zeng, Y.; Fan, C.; Zou, S.; Zhang, Y.; Li, P.; et al. Exendin-4 Improves Diabetic Kidney Disease in C57BL/6 Mice Independent of Brown Adipose Tissue Activation. *J. Diabetes Res.* **2020**, *2020*, 9084567. [CrossRef] [PubMed]
85. Zhao, J.; He, K.; Du, H.; Wei, G.; Wen, Y.; Wang, J.; Zhou, X.; Wang, J. Bioinformatics prediction and experimental verification of key biomarkers for diabetic kidney disease based on transcriptome sequencing in mice. *PeerJ* **2022**, *10*, e13932. [CrossRef] [PubMed]
86. Jung, J.H.; Choi, J.E.; Song, J.H.; Ahn, S.H. Human CD36 overexpression in renal tubules accelerates the progression of renal diseases in a mouse model of folic acid-induced acute kidney injury. *Kidney Res. Clin. Pract.* **2018**, *37*, 30–40. [CrossRef] [PubMed]
87. Ma, Y.; Huang, L.; Zhang, Z.; Yang, P.; Chen, Q.; Zeng, X.; Tan, F.; Wang, C.; Ruan, X.; Liao, X. CD36 promotes tubular ferroptosis by regulating the ubiquitination of FSP1 in acute kidney injury. *Genes Dis.* **2024**, *11*, 449–463. [CrossRef] [PubMed]

Disclaimer/Publisher's Note: The statements, opinions and data contained in all publications are solely those of the individual author(s) and contributor(s) and not of MDPI and/or the editor(s). MDPI and/or the editor(s) disclaim responsibility for any injury to people or property resulting from any ideas, methods, instructions or products referred to in the content.